Updates of stock assessment of Pacific saury (*Cololabis saira*) in the Western North Pacific Ocean through 2022

Jhen Hsu[1], Yi-Jay Chang[1], Chih-hao Hsieh[1], Wen-Bin Huang[2], Tung-Hsieh Chiang[3]

1. Institute of Oceanography, National Taiwan University

2. Department of Natural Resources and Environmental Studies, National Dong Hwa University

3. Overseas Fisheries Development Council of Chinese Taipei

Summary

This paper describes the updates of stock assessment of the Pacific saury (*Cololabis saira*) in the Western North Pacific Ocean (WNPO) based on the guideline of the 2021 SSC PS09. The assessment consisted of applying the Bayesian state-space surplus production model for estimating the biomass from 1980 to 2023 with available catches from 1980 to 2022. Abundance indices available for WNPO Pacific saury consisted of updated standardized catch-per-unit-effort (CPUE) of stick-held dip net fisheries from Japan (1980 – 2022), Chinese Taipei (2001 – 2022), Russia (1994 – 2021), Korea (2001 – 2022), and China (2013 – 2022), joint CPUE index (1994 – 2022) and biomass survey from Japan (2003 – 2023). Two base case models were considered for the assessment outputs. The results of two base case models indicated that the estimated biomass had a similar trend over years. The ensemble time-series of biomass is estimated to have an increasing pattern since 2000 with two peaks in 2003 and 2005, after then dramatically decreased overtime and below B_{MSY} in 2009 – 2022. It should be noted that the models estimate the lowest biomass level in 2020 and 2021 (median B_{2020}/B_{MSY} = 0.25, 80 percentile range 0.18 – 0.36; median B_{2021}/B_{MSY} = 0.25, 80 percentile range 0.18 – 0.37) and following a slight increase in 2022 and 2023 (median B_{2022}/B_{MSY} = 0.32, 80 percentile range 0.22 – 0.47; median B_{2023}/B_{MSY} = 0.42, 80 percentile range 0.26 - 0.66). In the recent three years (2021 – 2023), the biomass was estimated below the B_{MSY} (median $B_{2021-2023}/B_{MSY}$ = 0.34, 80 percentile range 0.23 – 0.49). A steady increase in fishing mortality is estimated to have occurred from 2004 to 2018, but a decrease trend in fishing mortality was found from 2020 to 2022, and the recent average fishing mortality is estimated to be above F_{MSY} (median $F_{2020-2022}/F_{MSY}$ = 1.08, 80 percentile range = 0.78 – 1.51). The ensemble MCMC results from the two base cases indicated that the 2022 stock status is likely within the yellow quadrant (Prob [$B_{2022}<B_{MSY}$ and $F_{2022}<F_{MSY}$] = 75%).

1. Introduction

Here, we present a preliminary stock assessment of Pacific saury in the WNPO of the North Pacific Fisheries Commission (NPFC) convention area through 2022. The assessment consisted of applying the Bayesian state-space surplus production model with available catches and standardized catch-per-unit-effort (CPUE) indices from the members from 1980 to 2022 and

the Japanese biomass index from 2003-2023. The Bayesian method provided direct estimates of the uncertainty of the model parameters and management quantities.

2. Material and methods

Fishery catch data from 1950 – 2022 for assessing WNPO saury were taken from the most recent summary of available fishery-dependent data. The commercial catch of Pacific saury caught by Japan, Chinese Taipei, Korea, China, Russia and other members in the WNPO area were collected from 1950 to 2022 (**Figure 1**). Estimates of standardized fishery-dependent catch-per-unit-effort (CPUE) of WNPO saury were available for Japan, Chinese Taipei, Korea, Russia, and China. Joint CPUE index was available from 1994 – 2022. Fishery-independent biomass index was available from Japanese scientific research surveys from 2003 – 2023 by using mid-water trawl (**Figure 2**). Comparison of input catch, standardized CPUE indices, and survey index between 2022 and 2023 for the Pacific saury assessment model was shown in Figure 3. Based on the SSC PS09 recommended base case scenarios (NPFC-2022-SSC PS09-Final Report), the model specification was shown in **Table 1**. The Bayesian analysis requires prior probability distributions for each of the model parameters. These priors were summarized in **Table 2**.

In addition, retrospective analysis was conducted to examine the consistency among successive model estimates of population size, or related assessment variables obtained as new data are gathered. Within-model retrospective analysis which trims the most recent 5 years of data in successive model runs were used to examine changes in the estimates of exploitable biomass. Modified Mohn's (1999) DR statistic was calculated as (Hurtado-Ferro et al., 2015):

$$DR = \frac{1}{npeels} \times \frac{X_{Y-y,tip} - X_{Y-y,ref}}{X_{Y-y,ref}}$$

where X denotes B, B/B$_{MSY}$, F, and F/F$_{MSY}$, y denotes year, *npeels* denotes the number of years that are dropped in successive fashion and the assessment rerun, Y is the last year in the full time series, *tip* denotes the terminal estimate from an assessment with a reduced time series, and *ref* denotes the assessment using the full time series.

3. Results

3.1 Convergence of base case and sensitivity models

The visual inspection of trace plots of the major parameters showed the good mixing of the three chains (i.e., moving around the parameter space), also indicative of convergence of the MCMC chains. It indicated that the posterior distributions of the model parameters were adequately sampled with the MCMC simulations.

3.2 Model fits to catch-per-unit-effort indices

Plots of residual diagnostics by fishery for the base and sensitivity case models were shown in **Figures 4 -5 and Figures A1 – A2**. For base case 1 and sensitivity case 1, models fit to the Chinese Taipei index had a residual trend with negative residuals in 2002 – 2010 and positive residuals in 2011 – 2022 (**Figure 4 and Figure A1**). The base model 2 and sensitivity case 2 fits to all CPUE indices did not have residual patterns over years (**Figure 5 and Figure A2**).

3.3 Posterior estimates of model parameters

Plots of posterior densities of the parameters r (intrinsic growth rate), K (carrying capacity), M (shape parameter), σ^2 (observation error), τ^2 (process error), b (Hyper-depletion/stability), and P_1 (biomass depletion in 1980) for each base and sensitivity cases were shown in **Figures 6 – 7 and Figures A3 – A4**. Summaries of parameter estimates of each of the base and sensitivity cases were provided in **Tables 3 – 4 and Tables A1-A4**.

The time-series plots of process errors for the two base cases are shown in **Figures 8 and 9**. In general, the patterns of process error for both base cases were around 0 and exhibited fluctuations after 1994, coinciding with the addition of CPUE data. Notably, the process error pattern for both base cases tend to be higher than 0 in the mid-2000s, whereas they tend to be lower than 0 after 2015.

3.4 Stock assessment results

Time-series of exploitable biomass (B), the ratio of biomass to B_{MSY} (B/B_{MSY}) and the biomass depletion (B/K) within each base and sensitivity cases were provided in **Figure 10 and Figures A5 – A8**. Although similar trends in biomass were observed in the two base cases, base case 2 exhibited a larger scale of exploitable biomass than base case 1 before 2003. In the sensitivity cases, the inclusion of early Japanese CPUE had minimal influence on biomass estimates before 1994, and the subsequent estimations did not differ significantly from the base case. This suggested that the inclusion of early Japanese CPUE index has negligible effects on the overall biomass results. The summary of estimated reference points for both base and sensitivity cases were provided in **Tables 5-6** and **Tables A5-A6**.

The ensemble time-series of biomass from the two base cases is estimated to have an increasing pattern since 2000, with two peaks in 2003 and 2005, after then decreased overtime and below B_{MSY} in 2009 – 2022. It should be noted that the models estimate the lowest biomass level in 2020 and 2021(median B_{2020}/B_{MSY} = 0.25, 80 percentile range 0.18 – 0.36; median B_{2021}/B_{MSY} = 0.25, 80 percentile range 0.18 – 0.37) and following a slight increase in 2022 and 2023 (median B_{2022}/B_{MSY} = 0.32, 80 percentile range 0.22 – 0.47; B_{2023}/B_{MSY} = 0.42, 80 percentile range 0.26 – 0.66). In the recent three years (2021 – 2023), the biomass was estimated below the B_{MSY} (median $B_{2021-2023}/B_{MSY}$ = 0.34, 80 percentile range 0.23 – 0.49) (**Figure 11**).

Time-series of the fishing mortality (F) and the ratio of fishing mortality to (F/F_{MSY}) within two base cases and sensitivity cases were shown in **Figure 12 and Figures A9 – A12**. The fishing mortality trend in base cases 1 and 2 exhibited similarities, but the fishing mortality

in base case 1 was higher before 2003 compared to base case 2. This disparity is attributed to the lower estimated exploitable biomass in base case 1 in contrast to base case 2. In the sensitivity case, the fishing mortality trends aligned with their respective base cases.

The ensemble time-series of the fishing mortality ratio trend from two base cases was shown in **Figure 13**. The fishing mortality was below F_{MSY} before 2007, and then the fishing mortality increased above F_{MSY} and reached a high level in 2014 and 2018, respectively. A decreased trend in fishing mortality was found from 2020 to 2022, and the recent average fishing mortality is estimated to be above F_{MSY} (median $F_{2020-2022}/F_{MSY} = 1.08$, 80 percentile range 0.78 – 1.51). It should be noted that the models estimate a slightly decreasing in fishing mortality in 2022 (median $F_{2022}/F_{MSY} = 0.81$, 80 percentile range 0.55 – 1.24).

The quantities of management interest reference points from joint estimates of the base case 1 and 2 were shown in **Table 7**. Overall, the ensemble MCMC results from the two base cases indicated that the 2022 stock status is likely within the yellow quadrant (Prob [$B_{2022}<B_{MSY}$ and $F_{2022}<F_{MSY}$] = 75%) (**Figure 14**). The ensemble MCMC results from two base cases in the last year and the recent three years were also shown in **Figure 15**, and it suggested that the stock status of Pacific saury is located at the red quadrant in the recent three years. Additionally, the Kobe phase plot of stock status derived from the sensitivity cases indicated that considering Japanese early CPUE would have minimal impact on the saury's stock condition in recent years (**Figure A13**).

3.5 Retrospective analysis

Retrospective analyses for the two base cases showed that the time-series of B, B/B_{MSY}, F and F/F_{MSY} with the removal of most 5 years of data (catch: 2016 – 2020; Japan biomass survey: 2017 – 2021) in successive model runs match very well with the full time series assessment (**Figures 16 and 17**). The DR statistic metrics for each quantity range from -0.12 to 0.12 in base case 1 (**Figure 16**) and from -0.083 to 0.073 in base case 2 (**Figure 17**). These values fall within the range of -0.22 to 0.30, as the rule of thumb for shorter-lived species suggested by Hurtado-Ferro et al. (2015). This suggested that there is no consistent pattern of bias in the estimates of the terminal quantiles.

Table 1. Specifications of the two base case models and four sensitivity case models. "JPN_early" = early Japan (1980-1993), "JPN_late" = late Japan (1994-2022), "CT" = Chinese Taipei, "RUS" = Russia, "KOR" = Korea, "CHN" = China, "JPN_bio" = Japan biomass survey (NPFC-2022-SSC PS09-Final Report).

Model	Base case 1 (NB1)	Base case2 (NB2)	Sensitivity case1 (NS1)	Sensitivity case2 (NS2)
Initial year	— 1980			
Biomass survey	$$I_{bio,t} = q_{bio}B_t e^{v_{bio,t}}$$ $$V_{bio,t} \sim N(0, cv^2_{bio,t} + \sigma^2)$$ $$q_{bio} \sim U(0,1)(2003-2023)$$			
Fleet CPUEs and Joint CPUE	CHN (2013-2022) JPN_late (1994-2022) KOR (2001-2022) RUS (1994-2022) CT (2001-2022) $$I_{f,t} = q_f B_t^b e^{v_{f,t}}$$ $$v_{f,t} \sim N(0, \sigma_f^2)$$ $$\sigma_f^2 = c \bullet (ave(cv^2_{bio,t}) + \sigma^2)$$ where $ave(cv^2_{bio,t})$ is computed except for the 2020 biomass survey ($c=5$)	Joint CPUE (1994-2022) $$I_{joint,t} = q_{joint} B_t^b e^{v_{joint,t}}$$ $$v_{joint,t} \sim N(0, cv^2_{joint,t} + \sigma^2)$$	CHN (2013-2022) JPN_early (1980-1993, time-varying q) JPN_late (1994-2022) KOR (2001-2022) RUS (1994-2022) CT (2001-2022) $$I_{f,t} = q_f B_t^b e^{v_{f,t}}$$ $$v_{f,t} \sim N(0, \sigma_f^2)$$ $$\sigma_f^2 = c \bullet (ave(cv^2_{bio,t}) + \sigma^2)$$ where $ave(cv^2_{bio,t})$ is computed except for the 2020 biomass survey ($c=6$)	JPN_early (1980-1993, time-varying q) $$I_{JE,t} = q_{JE} B_t^b e^{v_{JE,t}}$$ $$v_{JE,t} \sim N(0, \sigma^2_{JE})$$ $$\sigma^2_{JE} = c \bullet (ave(cv^2_{joint,t}) + \sigma^2)$$ Joint CPUE (1994-2022) $$I_{joint,t} = q_{joint} B_t^b e^{v_{joint,t}}$$ $$v_{joint,t} \sim N(0, cv^2_{joint,t} + \sigma^2)$$
Hyper-depletion/ stability	A common parameter for all fisheries with a prior distribution, $b \sim U(0, 1)$		A common parameter for all fisheries but JPN_early, with a prior distribution, $b \sim U(0, 1)$ [b for JPN_early is fixed at 1]	$b \sim U(0, 1)$ for joint CPUE. [b for JPN_early is fixed at 1]
Prior for other than q_{bio}	Own preferred options			

Table 2. Summary of the specified priors for the Bayesian state-space models. "JPN1" = early Japan (1980 – 1993), "JPN2" = late Japan (1994 – 2022), "CT" = Chinese Taipei, "RUS" = Russia, "KOR" = Korea, "CHN" = China, "JPN_bio" = Japan biomass survey.

Parameter	Description	Prior
K	Carrying capacity (10,000 mt)	$K \sim \log N\left(\log(180) - \dfrac{\sigma_K^2}{2}, \sigma_K^2\right); CV_K = 2$
r	Intrinsic growth rate (year^{-1})	$r \sim \log N\left(\log(1.2) - \dfrac{\sigma_r^2}{2}, \sigma_r^2\right); CV_r = 2$
M	Shape parameter	$M \sim Gamma(2,2)$
q	Catchability for fleets (JPN2; CT; RUS; KOR; CHN and Joint CPUE)	$1/q \sim Gamma(0.01, 0.01)$
q_{bio}	catchability for Japanese survey biomass	$q_{bio} \sim U(0,1)$
q_{JPN1}^{1980}	Time-varying catchability for JPN1 in 1980	$q_{JPN1}^{1980} \sim U(1 \times 10^{-1}, 1)$
ω	Annual deviation of log-scale time-varying catchability	$\omega \sim N(0, 0.1)$
β	Hyperstability of CPUE during 1994 - 2022	$\beta \sim U(0,1)$
σ^2	Common observation error of CPUE	$1/\sigma^2 \sim Gamma(2, 0.45)$
τ^2	Process error	$1/\tau^2 \sim Gamma(4, 0.1)$
P_1	Initial condition (B_1/K)	$P_1 \sim \log N\left(\log(0.6) - \dfrac{\sigma_{P_1}^2}{2}, \sigma_{P_1}^2\right); CV_{P_1} = 1$

Table 3. Summary of parameter estimates of the base case 1.

	Mean	Median	Lower 10th	Upper 10th
r	0.722	0.648	0.339	1.178
K	292.025	256.250	160.710	467.390
q_{CHN}	0.504	0.400	0.175	0.956
q_{JPN_late}	0.072	0.057	0.025	0.139
q_{KOR}	0.347	0.268	0.118	0.660
q_{RUS}	0.040	0.031	0.014	0.076
q_{CT}	0.079	0.060	0.027	0.149
q_{Bio}	0.502	0.487	0.272	0.754
M	1.086	0.962	0.374	1.959
obser_error	0.196	0.194	0.170	0.223
obser_error_survey	0.088	0.087	0.076	0.100
process_error	0.180	0.173	0.129	0.239
F_{MSY}	0.316	0.301	0.159	0.492
B_{MSY}	143.111	127.100	82.720	222.500
MSY	38.537	38.580	31.580	45.449
b	0.744	0.752	0.567	0.912

Table 4. Summary of parameter estimates of the base case 2.

Parameters	Mean	Median	Lower 10th	Upper 10th
r	0.684	0.612	0.284	1.157
K	305.397	265.400	157.310	513.680
q_{Bio}	0.508	0.485	0.258	0.799
q_{Joint}	0.065	0.049	0.407	2.122
M	1.178	1.035	0.016	0.132
obser_error	0.373	0.369	0.311	0.441
obser_error_survey	0.167	0.165	0.139	0.197
process_error	0.163	0.156	0.119	0.216
F_{MSY}	0.313	0.291	0.135	0.524
B_{MSY}	151.732	133.500	82.563	245.190
MSY	38.903	39.400	30.620	46.480
b	0.618	0.620	0.414	0.822

Table 5. Summary of reference points of the base case 1.

	Mean	Median	Lower 10th	Upper 10th
F_{2020_2022}	0.328	0.309	0.164	0.523
F_{2022}	0.241	0.228	0.125	0.375
F_{MSY}	0.316	0.301	0.159	0.492
MSY	38.537	38.580	31.580	45.449
F_{2022}/F_{MSY}	0.802	0.767	0.538	1.097
F_{2020_2022}/F_{MSY}	1.071	1.037	0.766	1.404
K	292.025	256.250	160.710	467.390
B_{2022}	50.207	43.940	26.661	80.149
B_{2023}	65.699	57.990	36.811	102.500
B_{2021_2023}	51.841	45.502	28.388	82.063
B_{MSY}	143.111	127.100	82.720	222.500
B_{MSY}/K	0.499	0.496	0.428	0.575
B_{2022}/K	0.178	0.173	0.118	0.244
B_{2023}/K	0.238	0.229	0.147	0.342
$B_{2021-2023}/K$	0.185	0.180	0.122	0.253
B_{2022}/B_{MSY}	0.357	0.343	0.244	0.485
B_{2023}/B_{MSY}	0.479	0.458	0.301	0.681
$B_{2021-2023}/B_{MSY}$	0.371	0.358	0.254	0.502

Table 6. Summary of reference points of the base case 2.

	Mean	Median	Lower 10th	Upper 10th
F_{2020_2022}	0.352	0.323	0.155	0.602
F_{2022}	0.268	0.249	0.124	0.440
F_{MSY}	0.313	0.291	0.135	0.524
MSY	38.903	39.400	30.620	46.480
F_{2022}/F_{MSY}	0.931	0.864	0.558	1.364
F_{2020_2022}/F_{MSY}	1.183	1.132	0.790	1.612
K	305.397	265.400	157.310	513.680
B_{2022}	47.750	40.275	22.761	80.716
B_{2023}	60.250	52.330	29.990	97.409
B_{2021_2023}	49.223	41.987	24.077	81.976
B_{MSY}	151.732	133.500	82.563	245.190
B_{MSY}/K	0.507	0.503	0.432	0.585
B_{2022}/K	0.161	0.153	0.100	0.231
B_{2023}/K	0.210	0.197	0.117	0.319
$B_{2021-2023}/K$	0.167	0.159	0.103	0.241
B_{2022}/B_{MSY}	0.318	0.300	0.203	0.456
B_{2023}/B_{MSY}	0.417	0.389	0.235	0.630
$B_{2021-2023}/B_{MSY}$	0.331	0.313	0.209	0.473

Table 7. Summary of joint estimates of reference points of the base cases 1 and 2.

	Mean	Median	Lower 10th	Upper 10th
$Catch_{2022}$	10.01	10.01	10.01	10.01
$F_{2020-2022}$	0.340	0.316	0.159	0.564
F_{2022}	0.255	0.237	0.124	0.408
F_{MSY}	0.314	0.297	0.147	0.507
MSY	38.720	38.940	31.093	46.020
F_{2022}/F_{MSY}	0.866	0.809	0.547	1.237
$F_{2020-2022}/F_{MSY}$	1.127	1.079	0.776	1.513
K	298.711	260.100	158.800	490.870
B_{2022}	48.979	42.300	24.510	80.487
B_{2023}	62.974	55.320	33.030	100.100
$B_{2021-2023}$	50.532	43.883	26.017	82.043
B_{MSY}	147.421	130.150	82.633	233.670
B_{MSY}/K	0.552	0.498	0.298	0.843
B_{2022}/K	0.169	0.163	0.107	0.239
B_{2023}/K	0.224	0.214	0.129	0.332
$B_{2021-2023}/K$	0.176	0.170	0.111	0.248
B_{2022}/B_{MSY}	0.338	0.323	0.219	0.474
B_{2023}/B_{MSY}	0.448	0.424	0.261	0.659
$B_{2021-2023}/B_{MSY}$	0.351	0.337	0.226	0.490
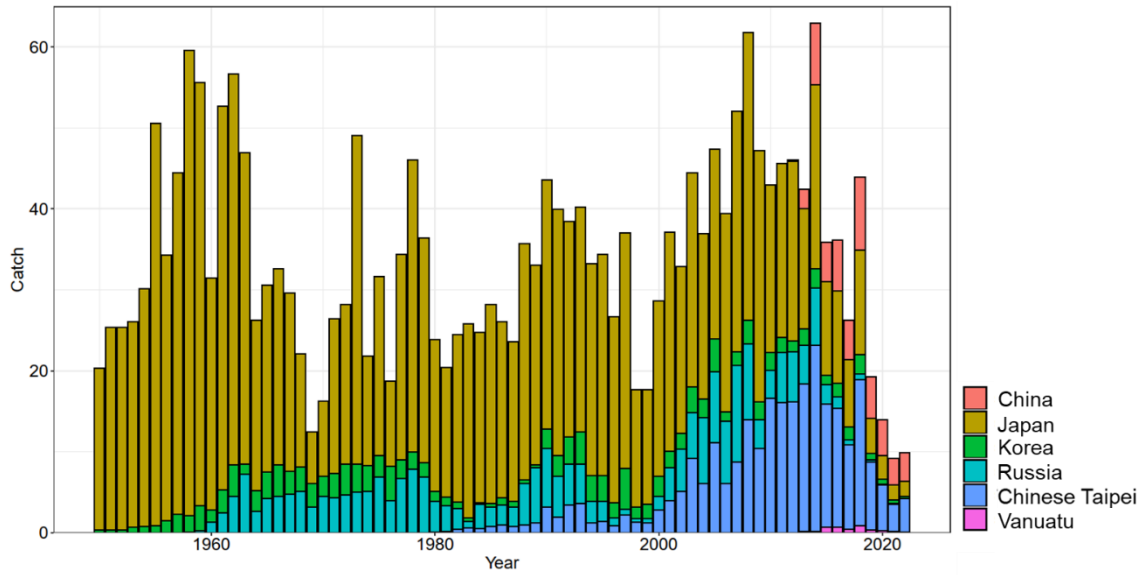
Figure 1. Time-series of Pacific saury historical catches by fleets during 1950 – 2022 in the Western North Pacific Ocean.
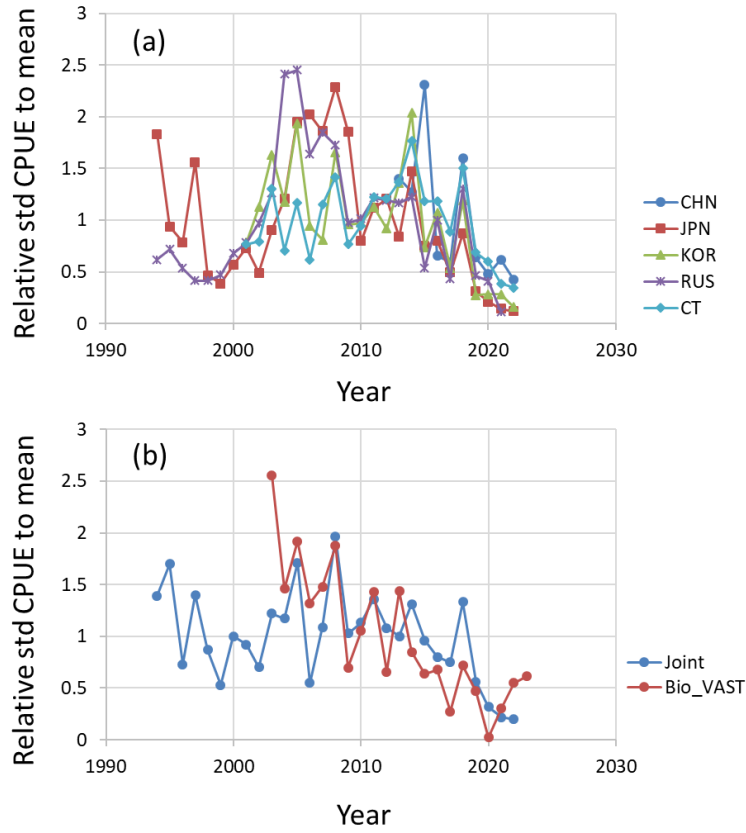
Figure 2. Time-series of (a) relative standardized CPUE indices by each member, and (b) relative joint CPUE index and fishery-independent biomass index.
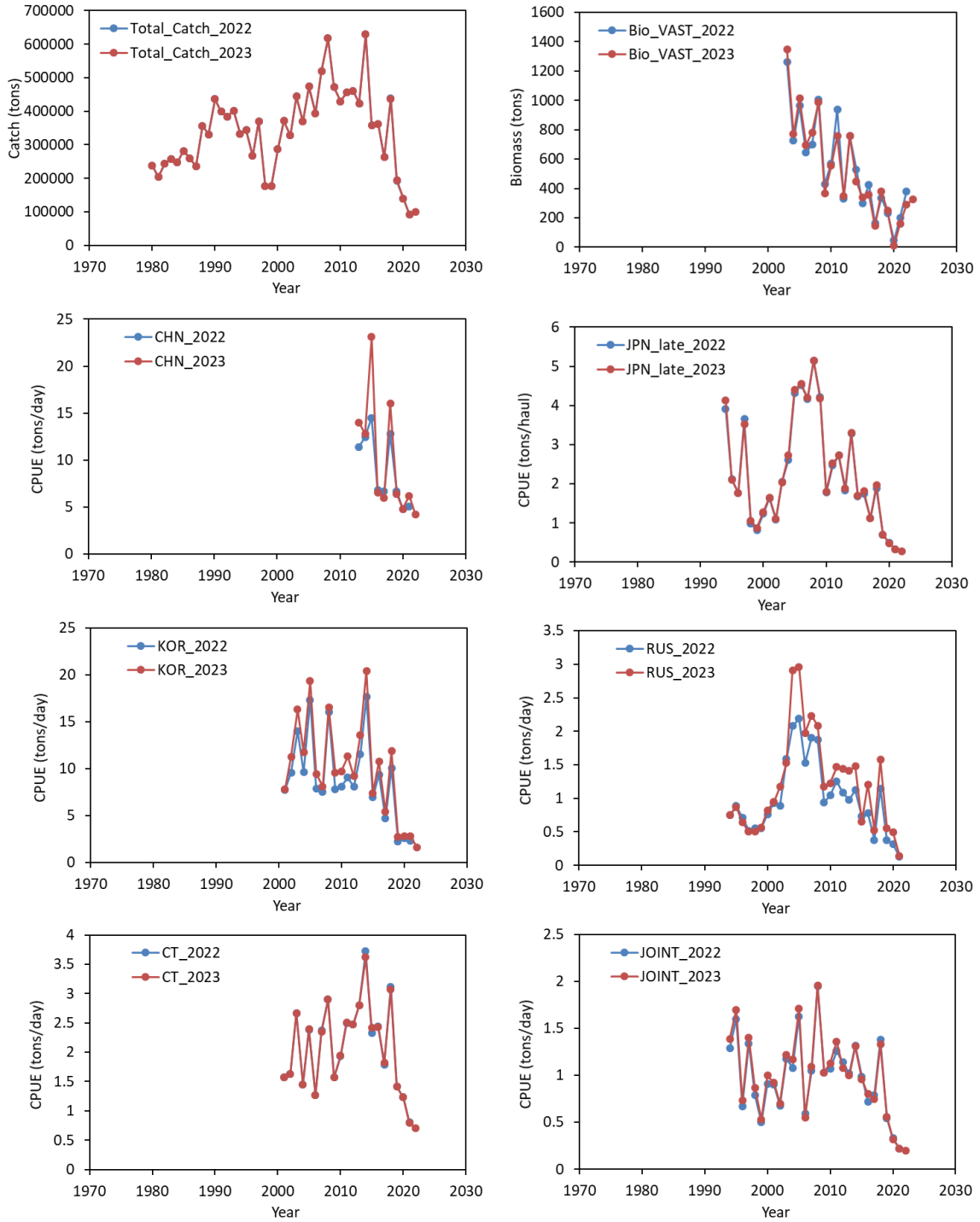
Figure 3. Comparison of input catch, standardized CPUE indices, and survey index between 2022 and 2023 for the Pacific saury assessment model.
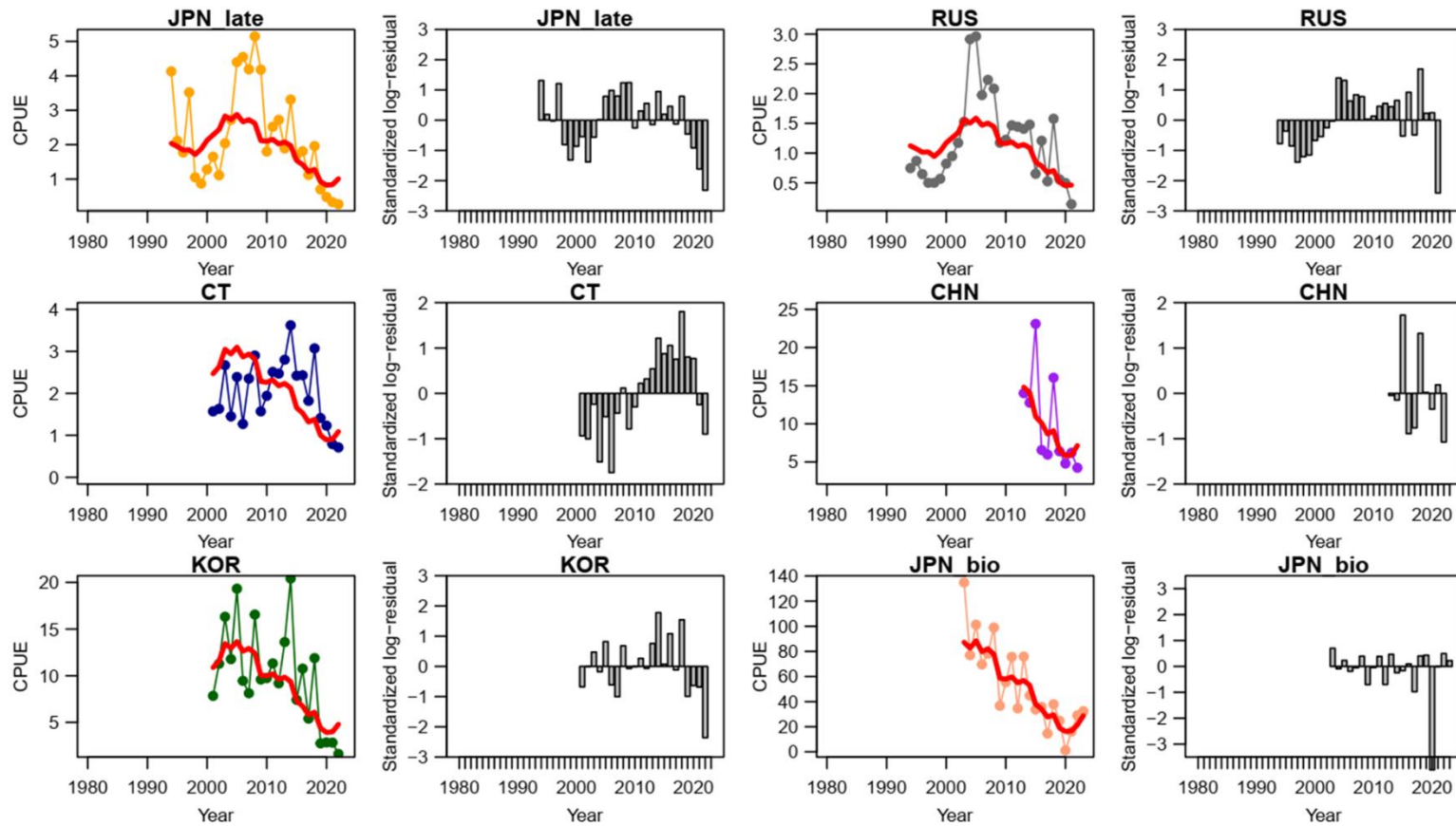
Figure 4. Time-series of observed (circle-line) and predicted (red solid line) catch per unit effort (CPUE) of Western North Pacific saury and standardized log-residuals for the base case 1 production model. "JPN_late" = late Japan (1994-2022), "CT" = Chinese Taipei, "RUS" = Russia, "KOR" = Korea, "CHN" = China, JPN_bio" = Japanese biomass survey.
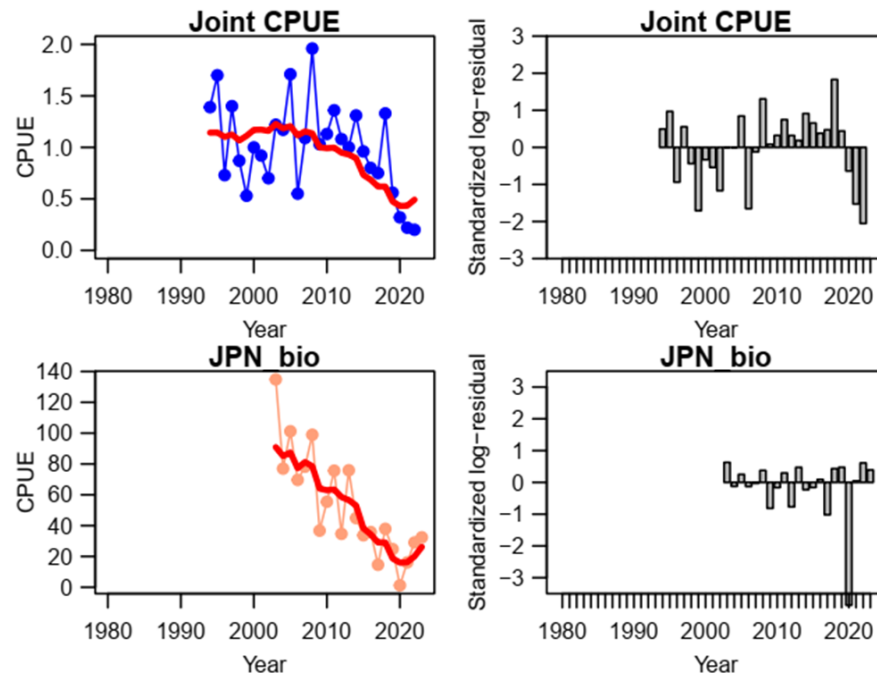
Figure 5. Time-series of observed (circle-line) and predicted (red solid line) catch per unit effort (CPUE) of Western North Pacific saury and standardized log-residuals for the base case 2 production model. "Joint CPUE" = joint CPUE index (1994 – 2022), and "JPN_bio" = Japanese biomass survey.
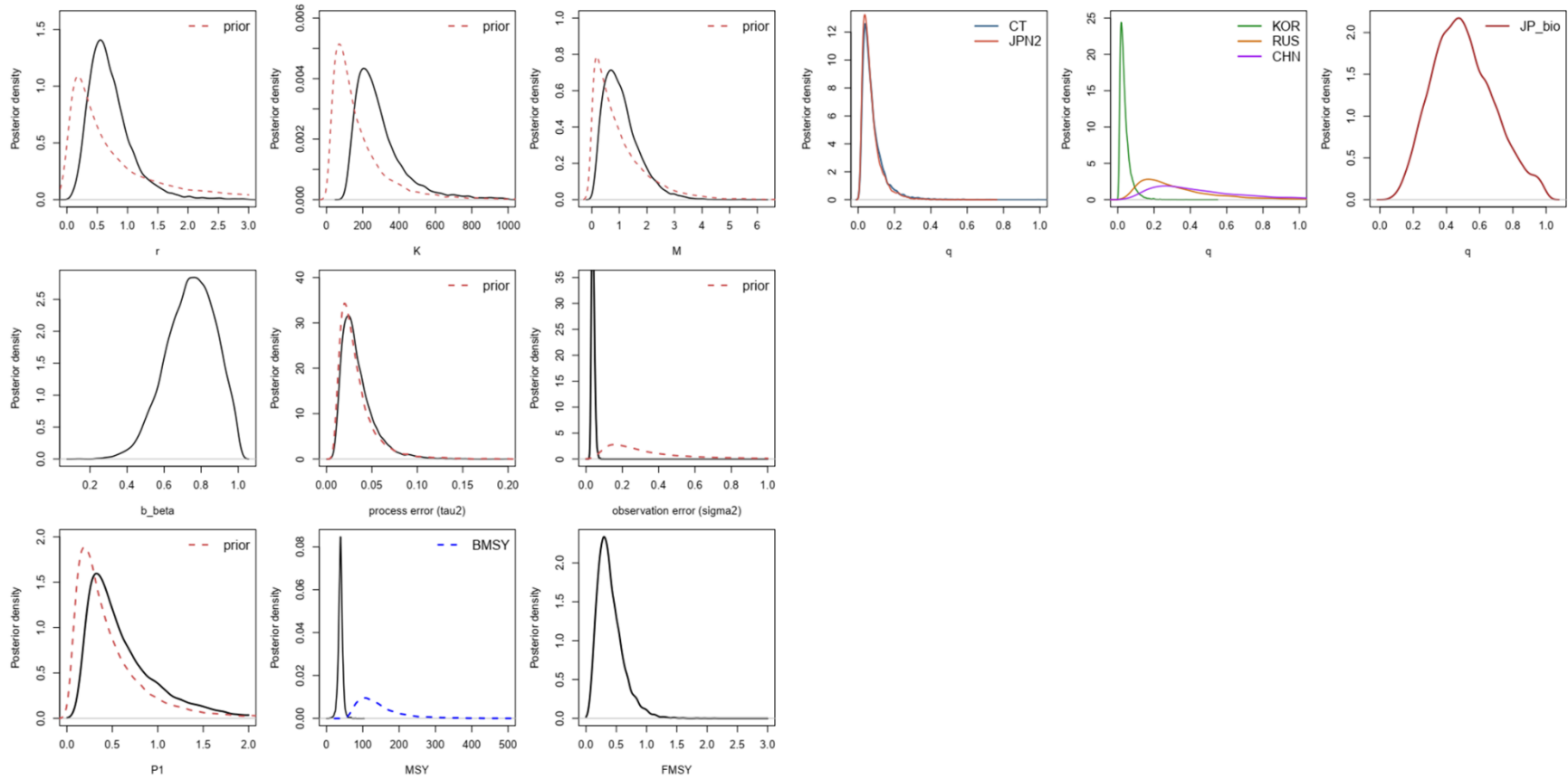
Figure 6. Kernel density estimates of the posterior distributions (solid lines) of various model parameters and management quantities for the base case 1 production model for the Pacific saury in the Western North Pacific Ocean. Proper prior densities are given by the dashed lines. "JPN2" = late Japan (1994-2022), "CT" = Chinese Taipei, "RUS" = Russia, "KOR" = Korea, "CHN" = China, "JP_bio" = Japanese biomass survey.
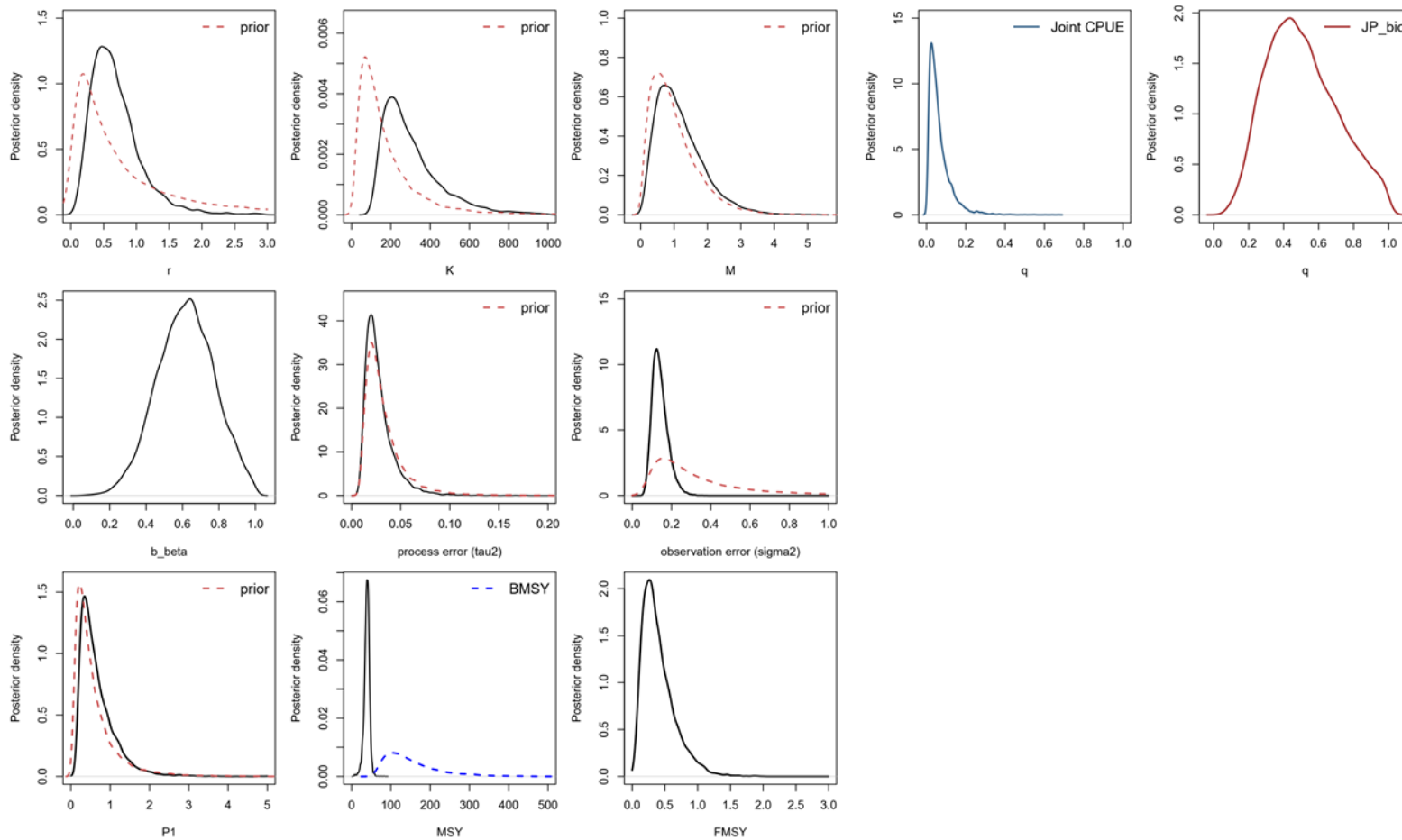
Figure 7. Kernel density estimates of the posterior distributions (solid lines) of various model parameters and management quantities for the base case 2 production model for the Pacific saury in the Western North Pacific Ocean. Proper prior densities are given by the dashed lines. "Joint CPUE" = Joint CPUE index, "JP_bio" = Japanese biomass survey.
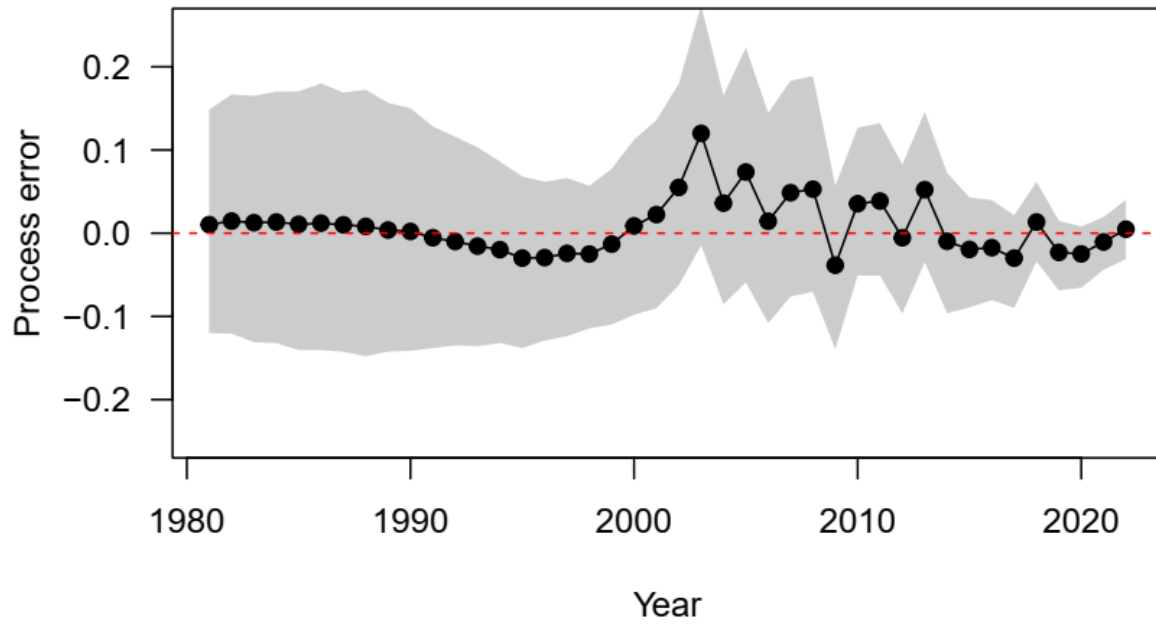
Figure 8. The time-series of the process error deviates on log-scale for base case 1. The polygon is the 80% confident interval.
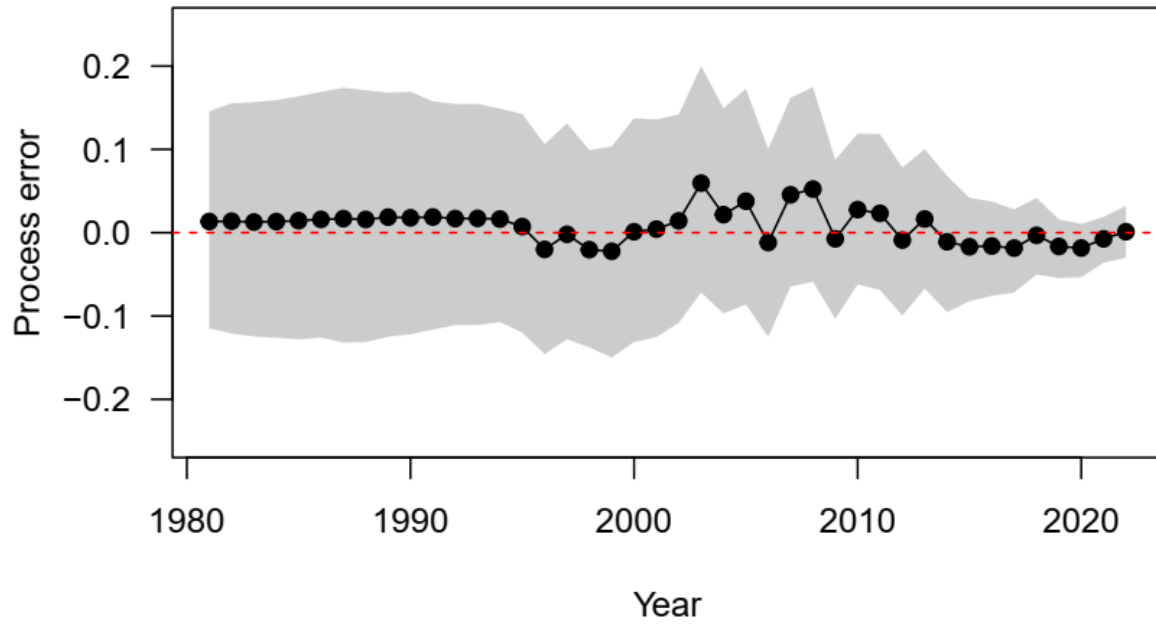
Figure 9. The time-series of the process error deviates on log-scale for base case 2. The polygon is the 80% confident interval.
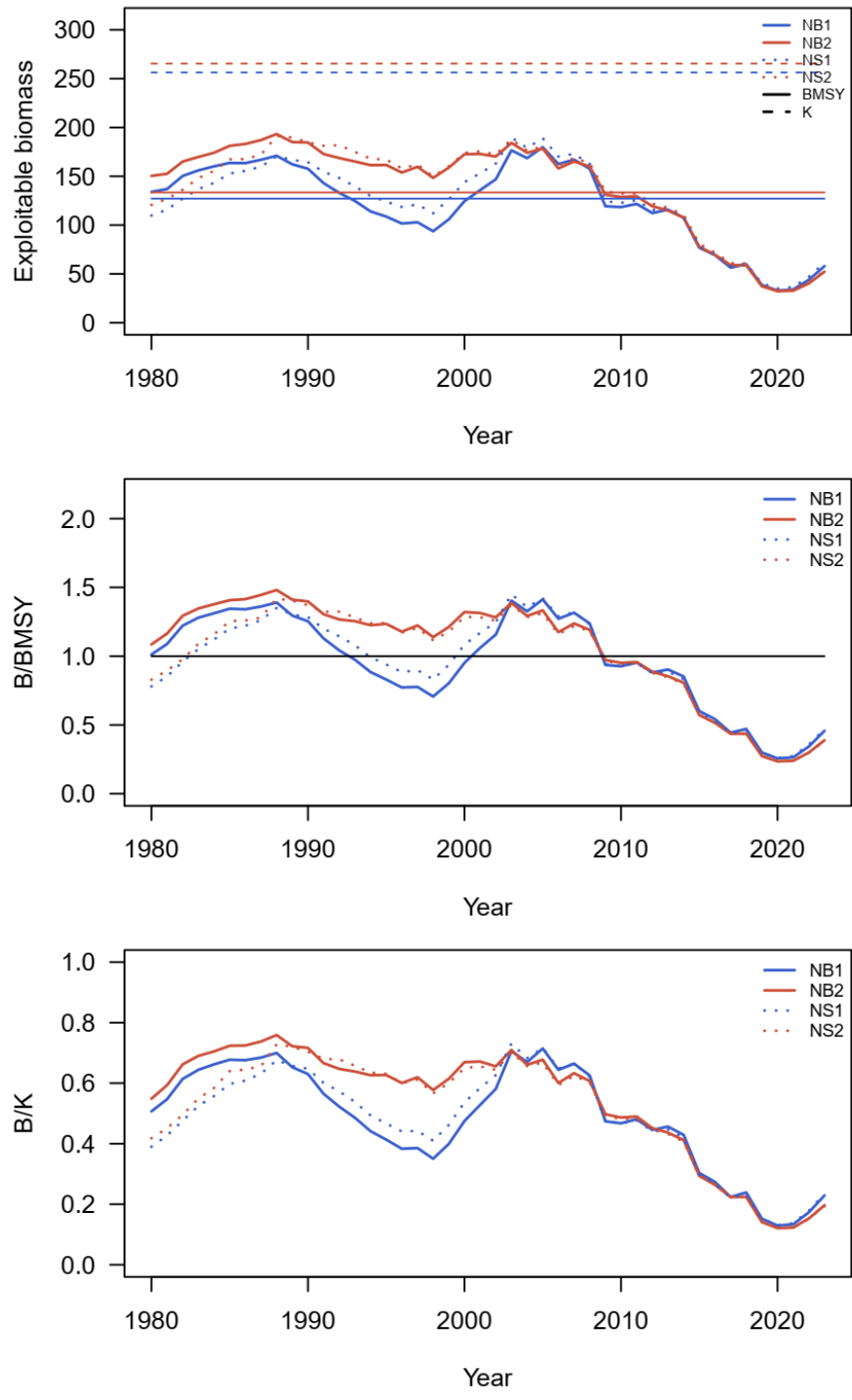
Figure 10. Time series of biomass (10,000 metric ton), the ratio of biomass to B_{MSY} (B/B_{MSY}), and the depletion ratio (B/K) of the western North Pacific saury for the base case 1-2 (NB1 and NB2) and sensitivity case 1-2 (NS1 and NS2).
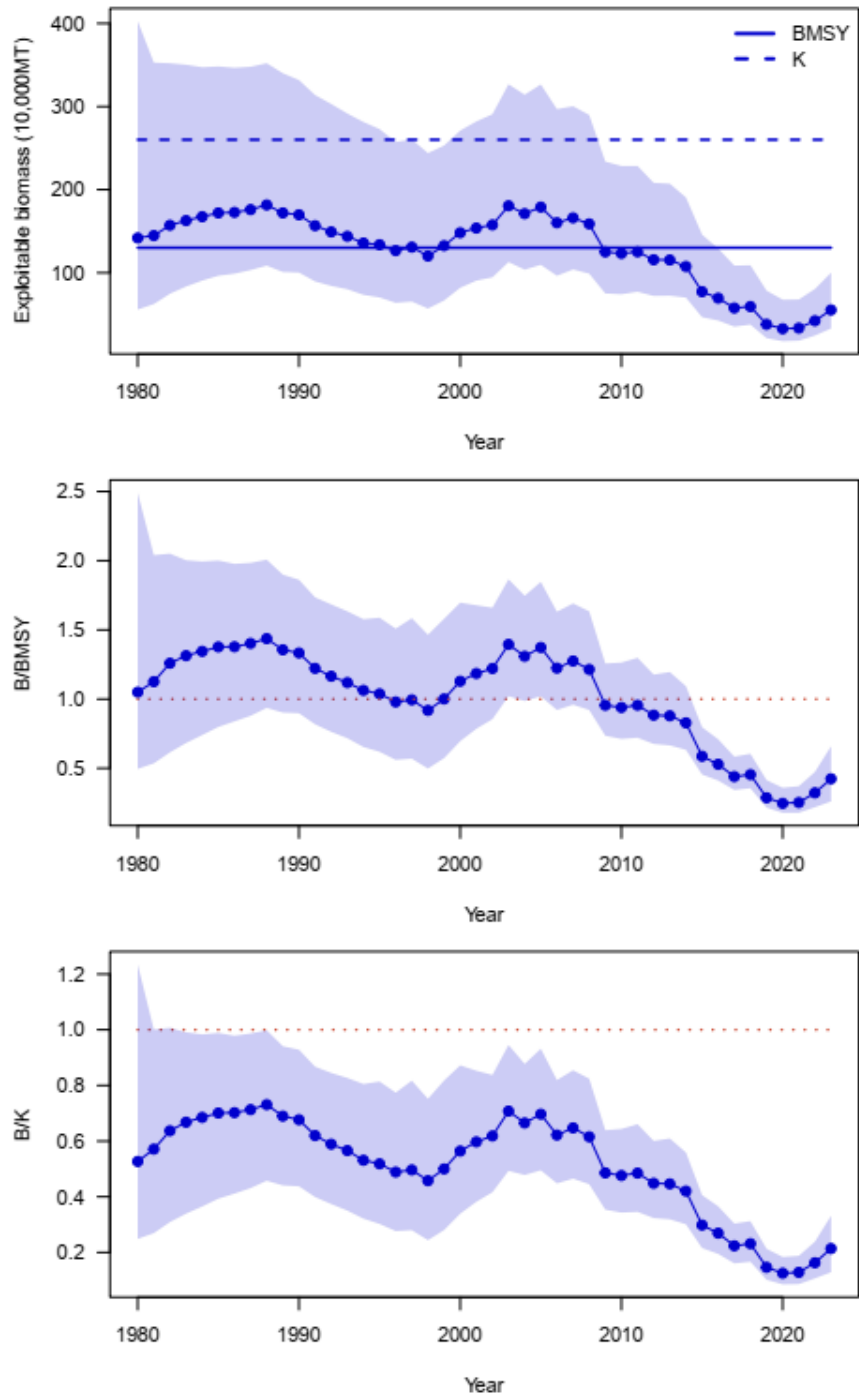
Figure 11. Time series of ensemble biomass (10,000 metric ton), the ratio of biomass to B_{MSY} (B/B_{MSY}), and the depletion ratio (B/K) of the western North Pacific saury for the median estimates of MCMC results from base cases 1-2.
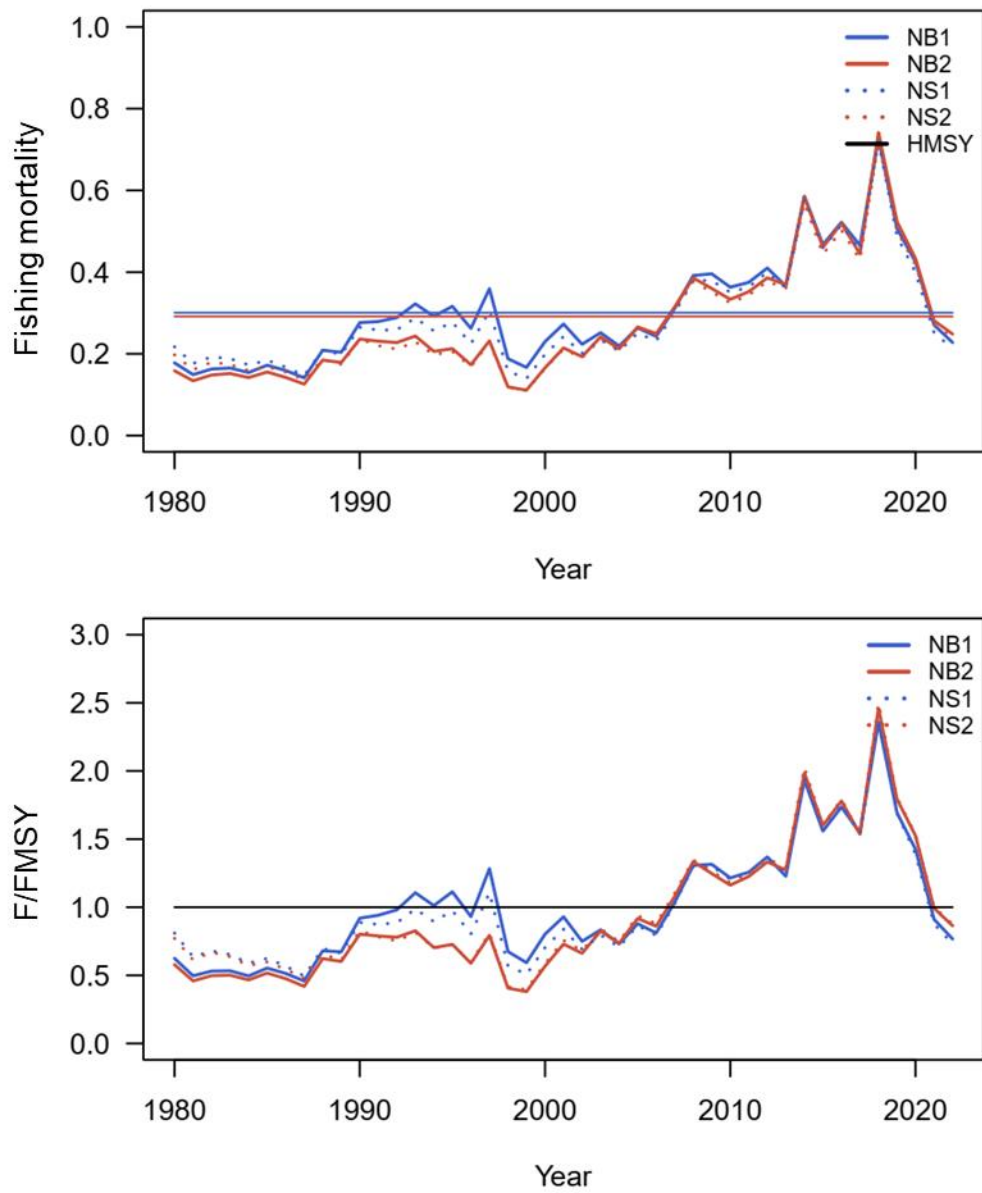
Figure 12. Time-series of fishing mortality (F) and the ratio of harvest rate to F_{MSY} (F/F_{MSY}) (b) of the western North Pacific saury for the base case 1-2 (NB1 and NB2) and sensitivity case 1-2 (NS1 and NS2).
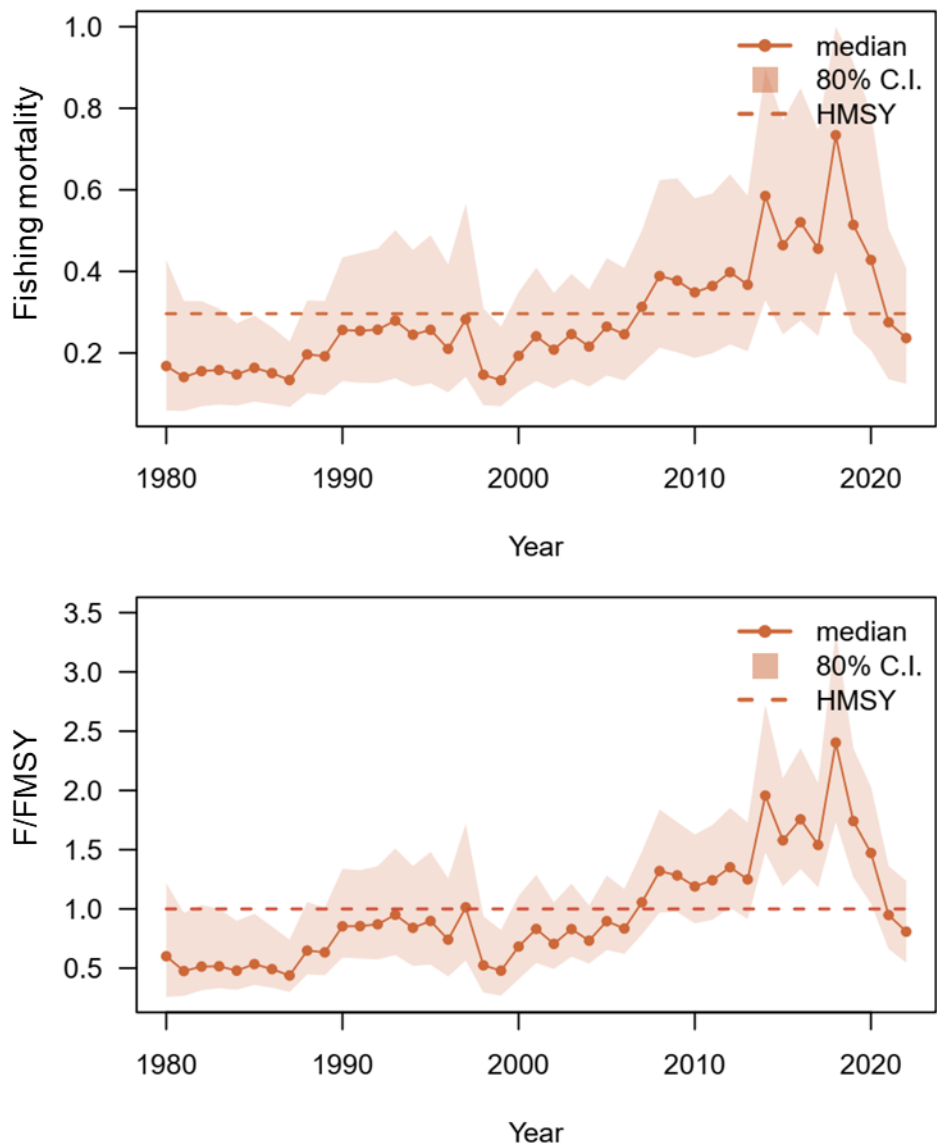
Figure 13. Time-series of fishing mortality and the ratio of fishing mortality to F_{MSY} (F/F_{MSY}) (b) of the western North Pacific saury for the median estimates of MCMC results from base cases 1 – 2.
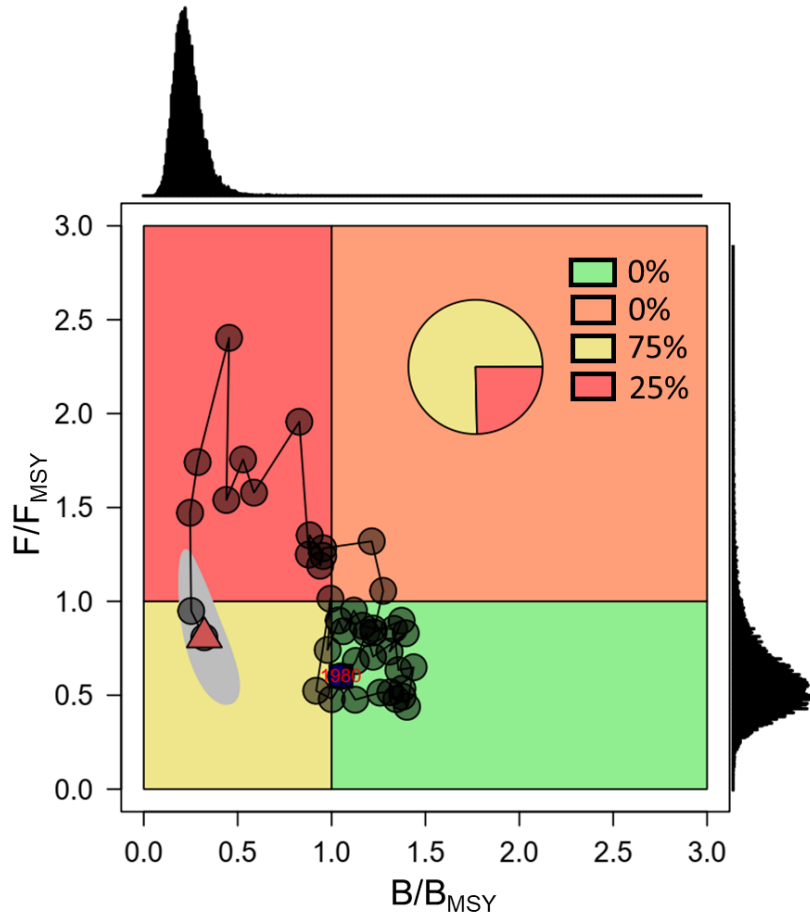
Figure 14. Ensemble Kobe phase plot of the stock trajectory of the western North Pacific saury from 1980 to 2022 (in a red triangle) with uncertainty estimate in 2022 (80% credible intervals, grey polygon) from the two base case models.
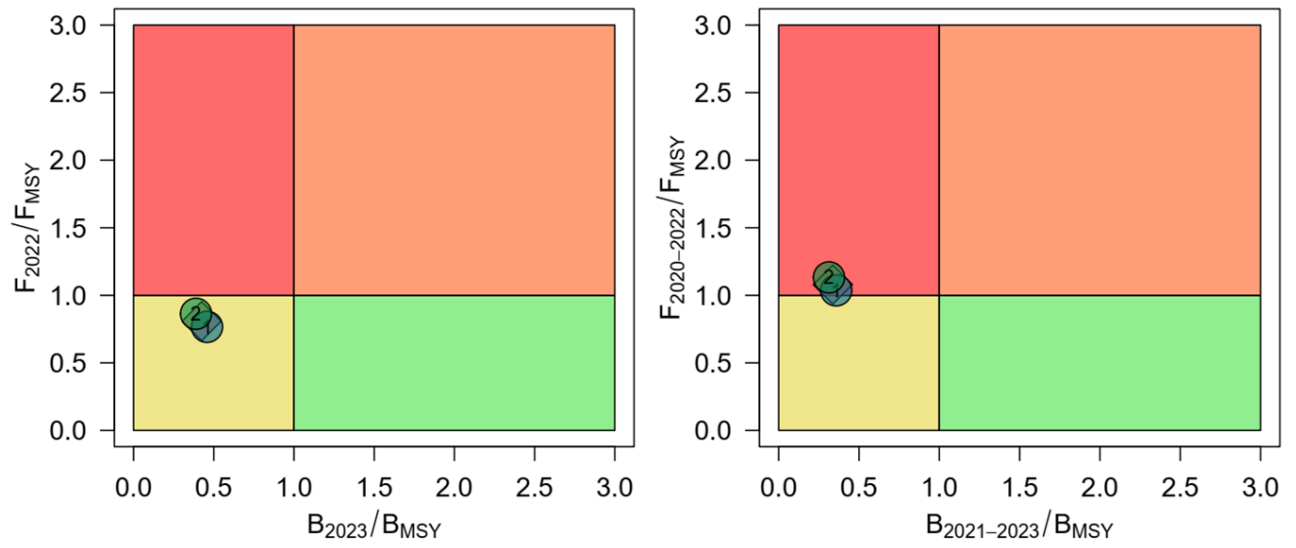
Figure 15. Kobe phase plot of stock status in the last year and recent three years ($B_{2021-2023}$ and $F_{2020-2022}$) of Pacific saury from the two base case models. The orange diamond is the median estimate of MCMC results from the two base case models.
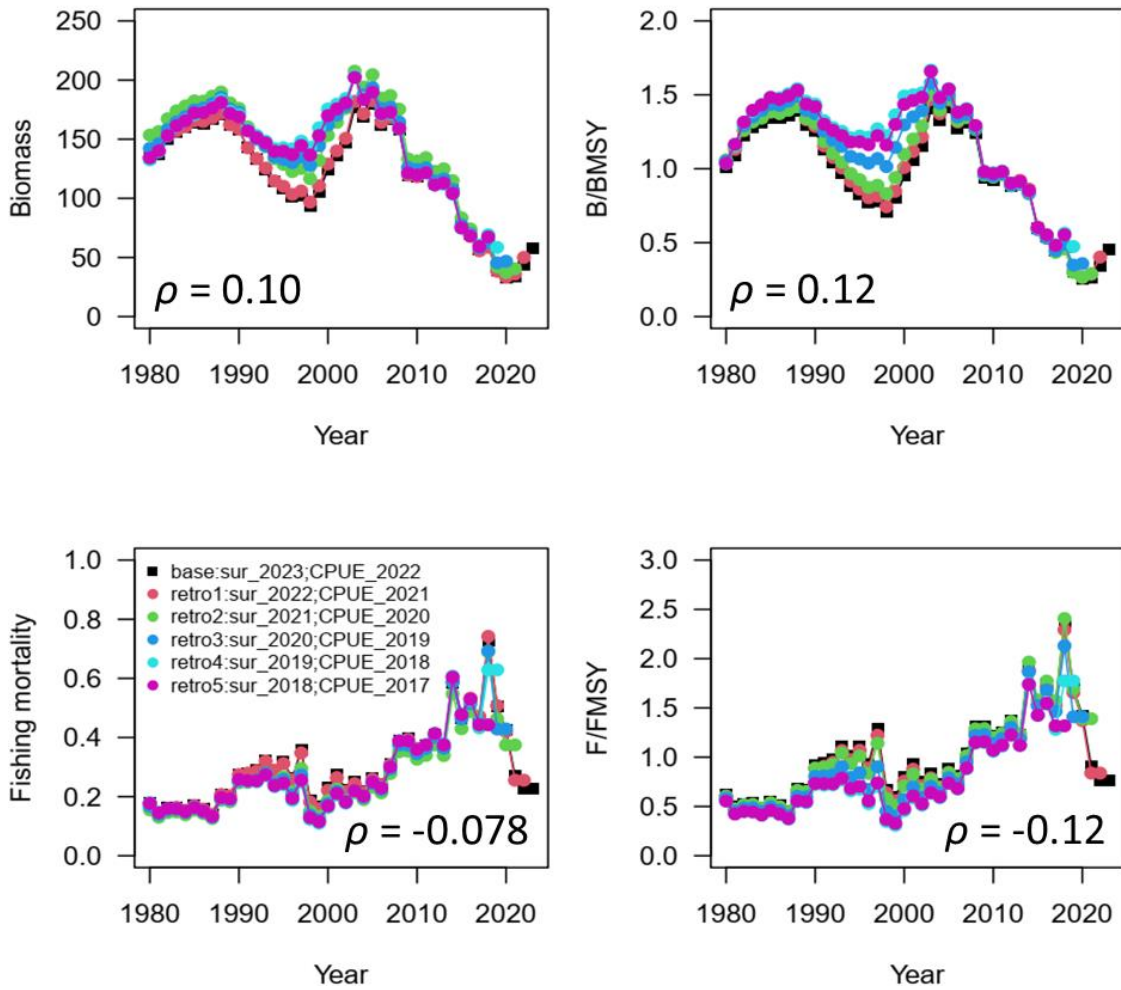
Figure 16. Five years within-model retrospective plots of the change in biomass, biomass to B_{MSY}, harvest rate and harvest rate to H_{MSY} of the western North Pacific saury from the base case 1.
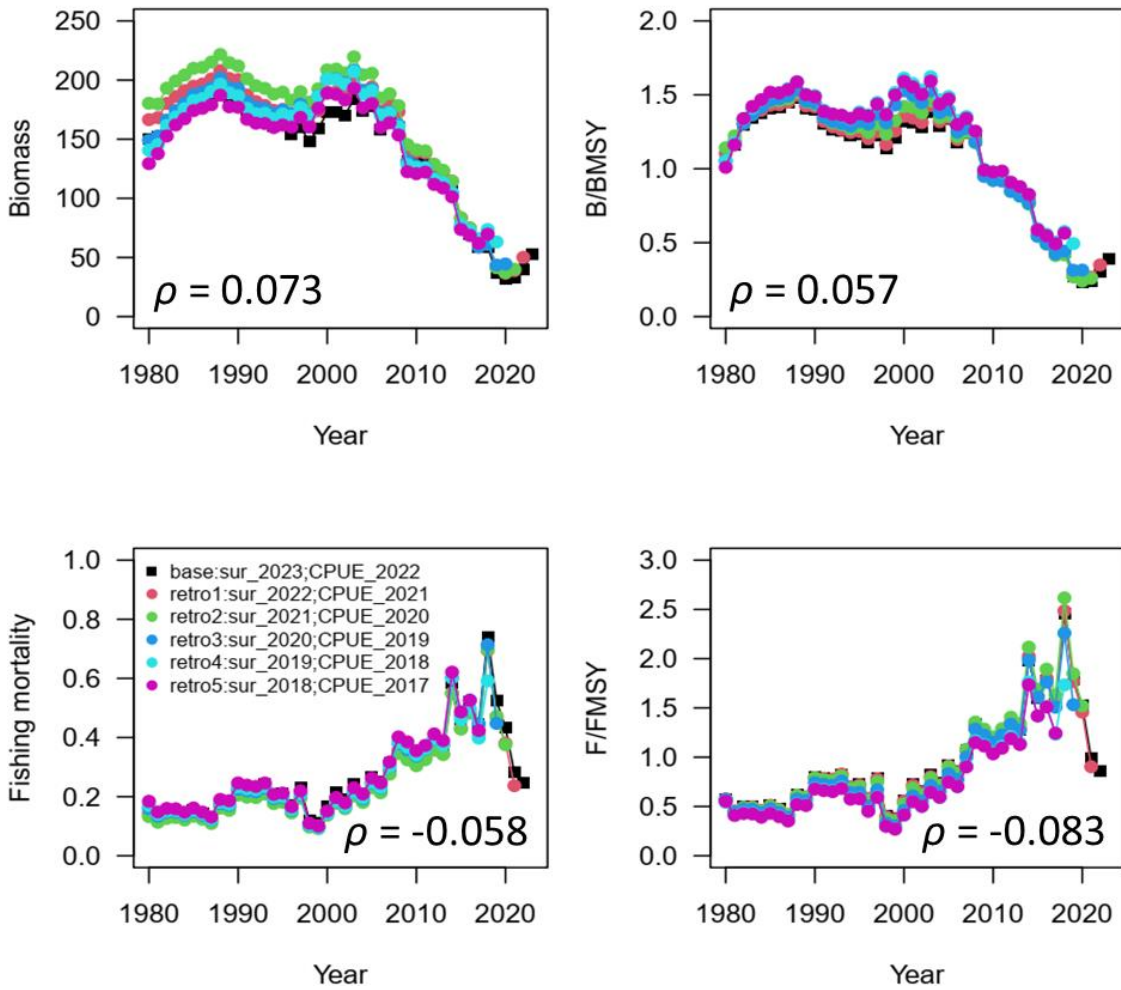
Figure 17. Five years within-model retrospective plots of the change in biomass, biomass to B_{MSY}, harvest rate and harvest rate to H_{MSY} of the western North Pacific saury from the base case 2.

Appendix tables

Table A1. Summary of parameter estimates of the sensitivity case 1.

	Mean	Median	Lower 10th	Upper 10th
r	0.715	0.638	0.330	1.181
K	303.378	266.550	168.010	484.900
q_{CHN}	0.592	0.454	0.185	1.166
q_{JPN_late}	0.085	0.063	0.026	0.165
q_{KOR}	0.412	0.305	0.124	0.824
q_{RUS}	0.047	0.035	0.015	0.093
q_{CT}	0.093	0.070	0.028	0.183
q_{Bio}	0.484	0.469	0.262	0.728
M	1.073	0.937	0.362	1.950
obser_error	0.186	0.184	0.162	0.211
obser_error_survey	0.083	0.082	0.072	0.094
process_error	0.171	0.164	0.123	0.228
F_{MSY}	0.307	0.292	0.156	0.476
B_{MSY}	148.415	131.600	86.002	231.900
MSY	38.903	38.850	32.070	45.810
b	0.708	0.714	0.518	0.894

Table A2. Summary of time-varying catchability for the JPN_early estimates of the sensitivity case 1.

Year	Mean	Median	Lower 10th	Upper 10th
1980	0.0077	0.006	0.0023	0.0149
1981	0.0074	0.0059	0.0024	0.0141
1982	0.0072	0.0059	0.0025	0.0135
1983	0.0077	0.0064	0.0028	0.0143
1984	0.0082	0.0069	0.0031	0.015
1985	0.0091	0.0078	0.0035	0.0161
1986	0.0097	0.0084	0.0039	0.0169
1987	0.0108	0.0094	0.0045	0.0187
1988	0.0129	0.0112	0.0054	0.0222
1989	0.0148	0.013	0.0062	0.0257
1990	0.0164	0.0144	0.0068	0.0283
1991	0.019	0.0166	0.0077	0.0329
1992	0.0213	0.0183	0.0082	0.0379
1993	0.0225	0.0189	0.0081	0.0418

Table A3. Summary of parameter estimates of the sensitivity case 2.

	Mean	Median	Lower 10th	Upper 10th
r	0.658	0.585	0.279	1.103
K	313.935	276.550	166.300	518.800
q_{Bio}	0.493	0.475	0.261	0.763
q_{Joint}	0.059	0.045	0.394	2.165
M	1.187	1.039	0.014	0.118
obser_error	0.349	0.346	0.294	0.409
obser_error_survey	0.156	0.155	0.132	0.183
process_error	0.160	0.154	0.118	0.211
F_{MSY}	0.297	0.278	0.139	0.487
B_{MSY}	156.223	139.250	87.001	250.100
MSY	38.747	39.150	31.052	45.999
b	0.637	0.633	0.436	0.846

Table A4. Summary of time-varying catchability for the JPN_early estimates of the sensitivity case 2.

Year	Mean	Median	Lower 10th	Upper 10th
1980	0.00675	0.00536	0.00201	0.01335
1981	0.00620	0.00494	0.00201	0.01204
1982	0.00567	0.00463	0.00200	0.01067
1983	0.00637	0.00536	0.00239	0.01164
1984	0.00682	0.00583	0.00268	0.01211
1985	0.00789	0.00696	0.00326	0.01352
1986	0.00815	0.00727	0.00343	0.01374
1987	0.00874	0.00787	0.00381	0.01468
1988	0.01152	0.01056	0.00518	0.01911
1989	0.01388	0.01262	0.00617	0.02303
1990	0.01452	0.01323	0.00639	0.02425
1991	0.01759	0.01590	0.00775	0.02967
1992	0.02046	0.01826	0.00896	0.03490
1993	0.02068	0.01849	0.00867	0.03532

Table A5. Summary of reference points of the sensitivity case 1.

	Mean	Median	Lower 10th	Upper 10th
$F_{2020\text{-}2022}$	0.309	0.289	0.151	0.497
F_{2022}	0.224	0.213	0.116	0.349
F_{MSY}	0.307	0.292	0.156	0.476
MSY	38.903	38.85	32.07	45.81
F_{2022}/F_{MSY}	0.763	0.731	0.51	1.049
F_{2020_2022}/F_{MSY}	1.03	1.003	0.729	1.354
K	303.378	266.55	168.01	484.9
B_{2022}	54.52	47.105	28.681	86.668
B_{2023}	70.515	61.63	39.211	109.7
B_{2021_2023}	56	48.597	30.404	88.413
B_{MSY}	148.415	131.6	86.002	231.9
B_{MSY}/K	0.498	0.494	0.426	0.574
B_{2022}/K	0.185	0.179	0.121	0.254
B_{2023}/K	0.245	0.235	0.149	0.35
$B_{2021\text{-}2023}/K$	0.191	0.185	0.125	0.261
B_{2022}/B_{MSY}	0.372	0.357	0.25	0.509
B_{2023}/B_{MSY}	0.493	0.471	0.307	0.704
$B_{2021\text{-}2023}/B_{MSY}$	0.384	0.37	0.259	0.523

Table A6. Summary of reference points of the sensitivity case 2.

	Mean	Median	Lower 10th	Upper 10th
F_{2020_2022}	0.338	0.312	0.154	0.562
F_{2022}	0.260	0.241	0.124	0.420
F_{MSY}	0.297	0.278	0.139	0.487
MSY	38.747	39.150	31.052	45.999
F_{2022}/F_{MSY}	0.944	0.876	0.573	1.352
F_{2020_2022}/F_{MSY}	1.192	1.138	0.797	1.613
K	313.935	276.550	166.300	518.800
B_{2022}	48.401	41.525	23.851	80.607
B_{2023}	60.766	52.970	31.400	97.240
B_{2021_2023}	49.911	42.920	25.250	82.218
B_{MSY}	156.223	139.250	87.001	250.100
B_{MSY}/K	0.507	0.504	0.430	0.587
B_{2022}/K	0.159	0.152	0.099	0.229
B_{2023}/K	0.205	0.194	0.116	0.309
$B_{2021-2023}/K$	0.165	0.157	0.102	0.237
B_{2022}/B_{MSY}	0.314	0.297	0.201	0.446
B_{2023}/B_{MSY}	0.407	0.385	0.233	0.612
$B_{2021-2023}/B_{MSY}$	0.326	0.309	0.206	0.463

Appendix figures A
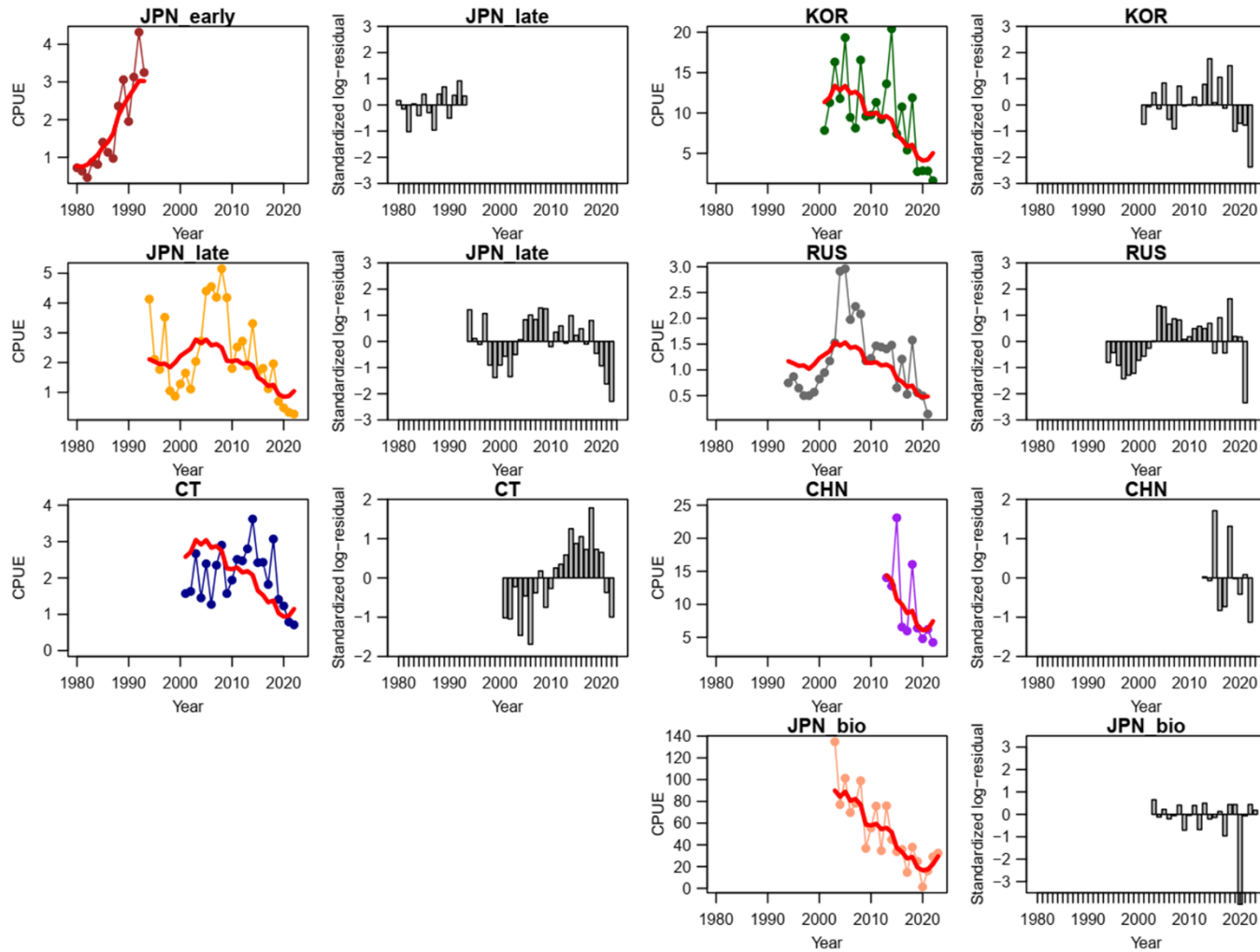
Figure A1. Time-series of observed (circle-line) and predicted (red solid line) catch per unit effort (CPUE) of Western North Pacific saury and standardized log-residuals for the base case 1 production model. "JPN_late" = late Japan (1994-2022), "CT" = Chinese Taipei, "RUS" = Russia, "KOR" = Korea, "CHN" = China, JPN_bio" = Japanese biomass survey.
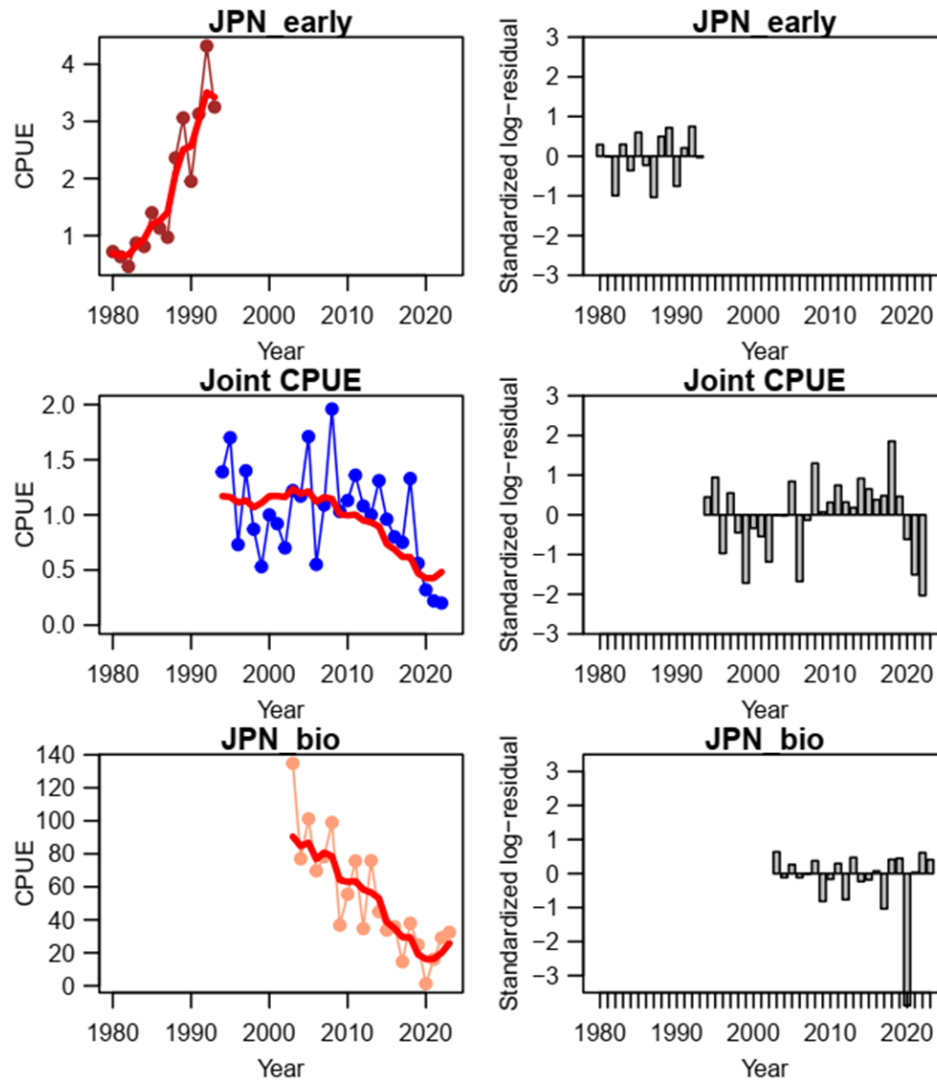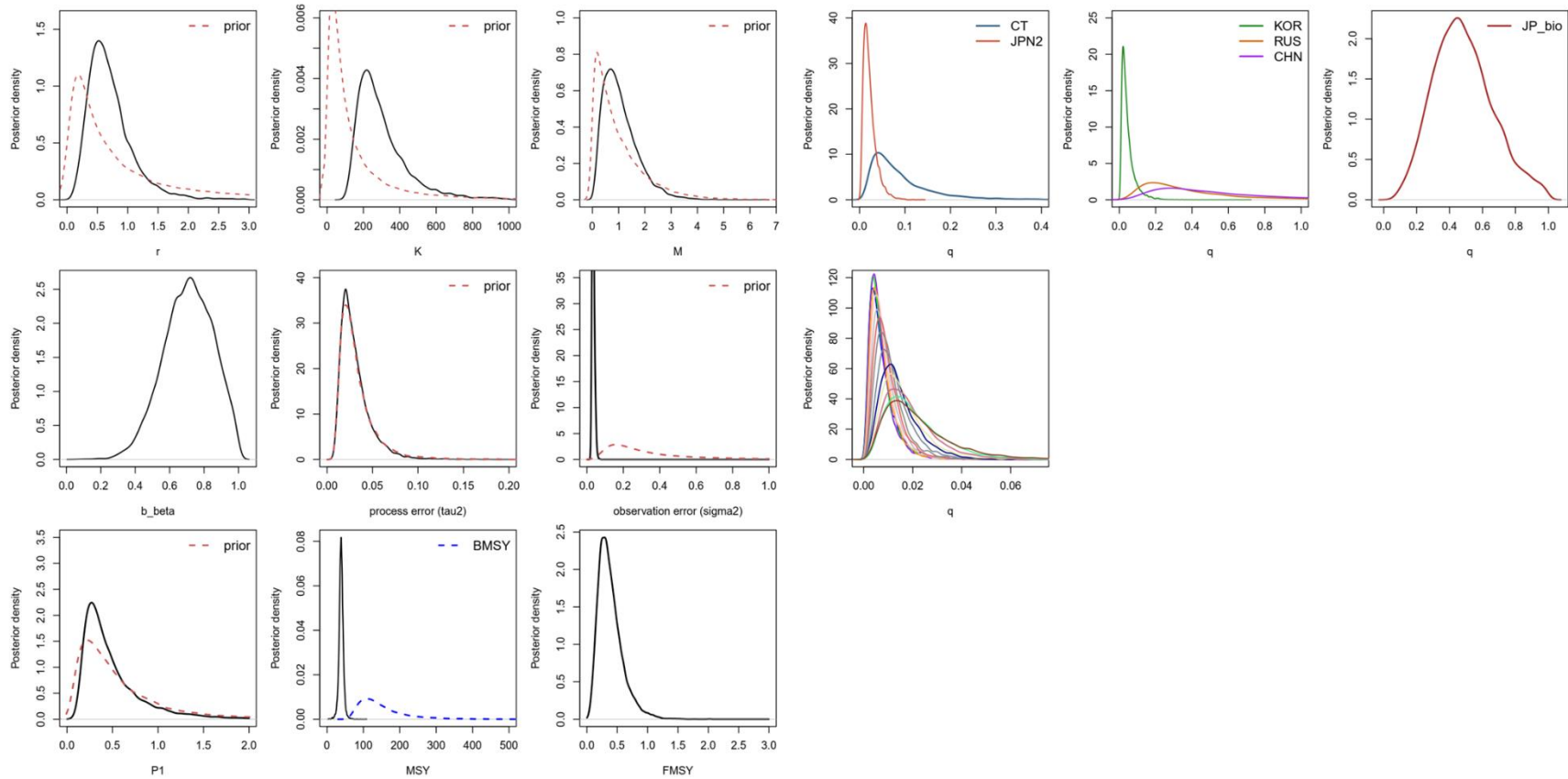
Figure A2. Time-series of observed (circle-line) and predicted (red solid line) catch per unit effort (CPUE) of Western North Pacific saury and standardized log-residuals for the base case 1 production model. "JPN_late" = late Japan (1994-2022), "CT" = Chinese Taipei, "RUS" = Russia, "KOR" = Korea, "CHN" = China, JPN_bio" = Japanese biomass survey.

Figure A3. Kernel density estimates of the posterior distributions (solid lines) of various model parameters and management quantities for the base case 1 production model for the Pacific saury in the Western North Pacific Ocean. Proper prior densities are given by the dashed lines. "JPN2" = late Japan (1994-2022), "CT" = Chinese Taipei, "RUS" = Russia, "KOR" = Korea, "CHN" = China, "JP_bio" = Japanese biomass survey.
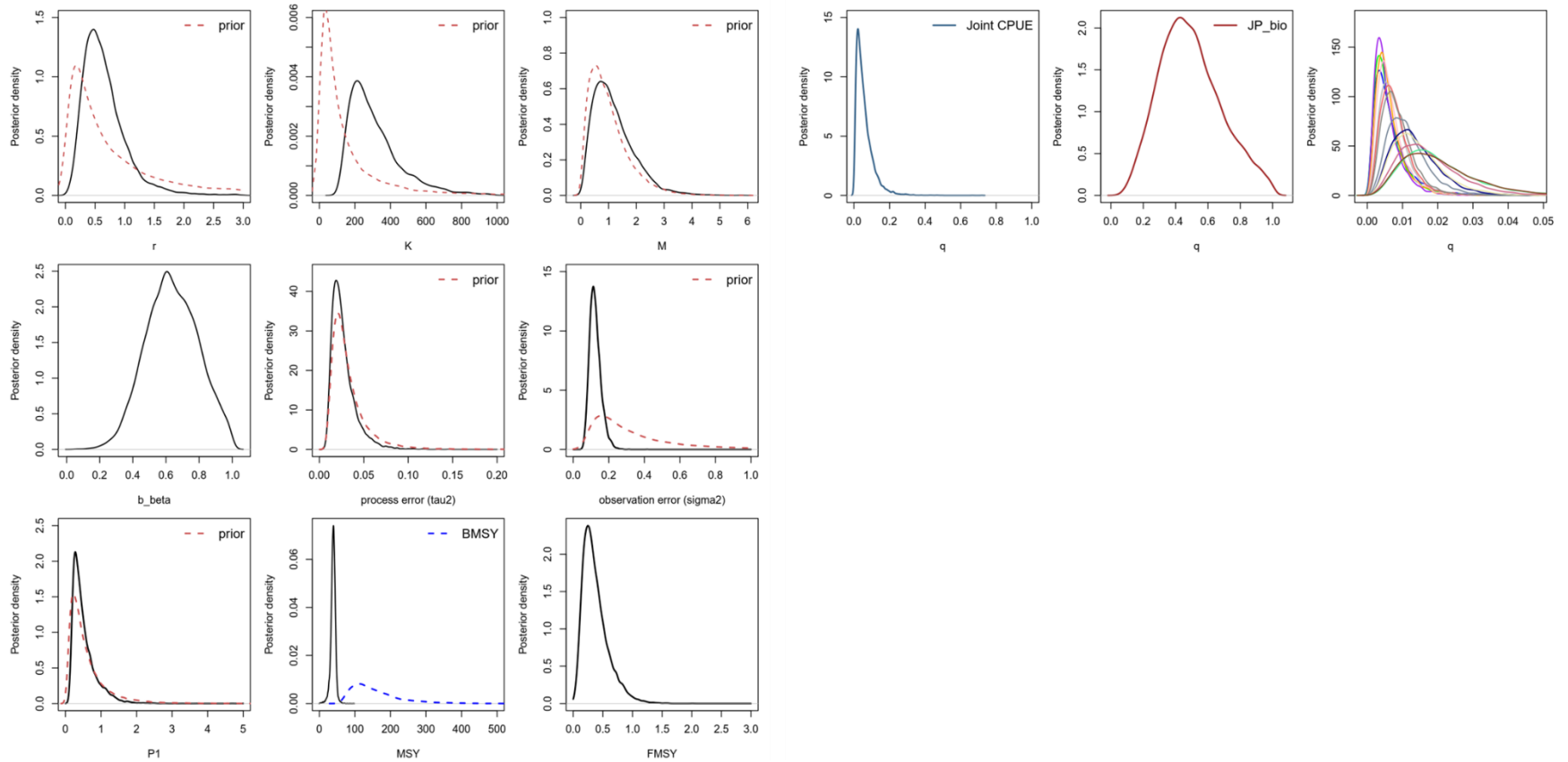
Figure A4. Kernel density estimates of the posterior distributions (solid lines) of various model parameters and management quantities for the base case 1 production model for the Pacific saury in the Western North Pacific Ocean. Proper prior densities are given by the dashed lines. "JPN2" = late Japan (1994-2022), "CT" = Chinese Taipei, "RUS" = Russia, "KOR" = Korea, "CHN" = China, "JP_bio" = Japanese biomass survey.
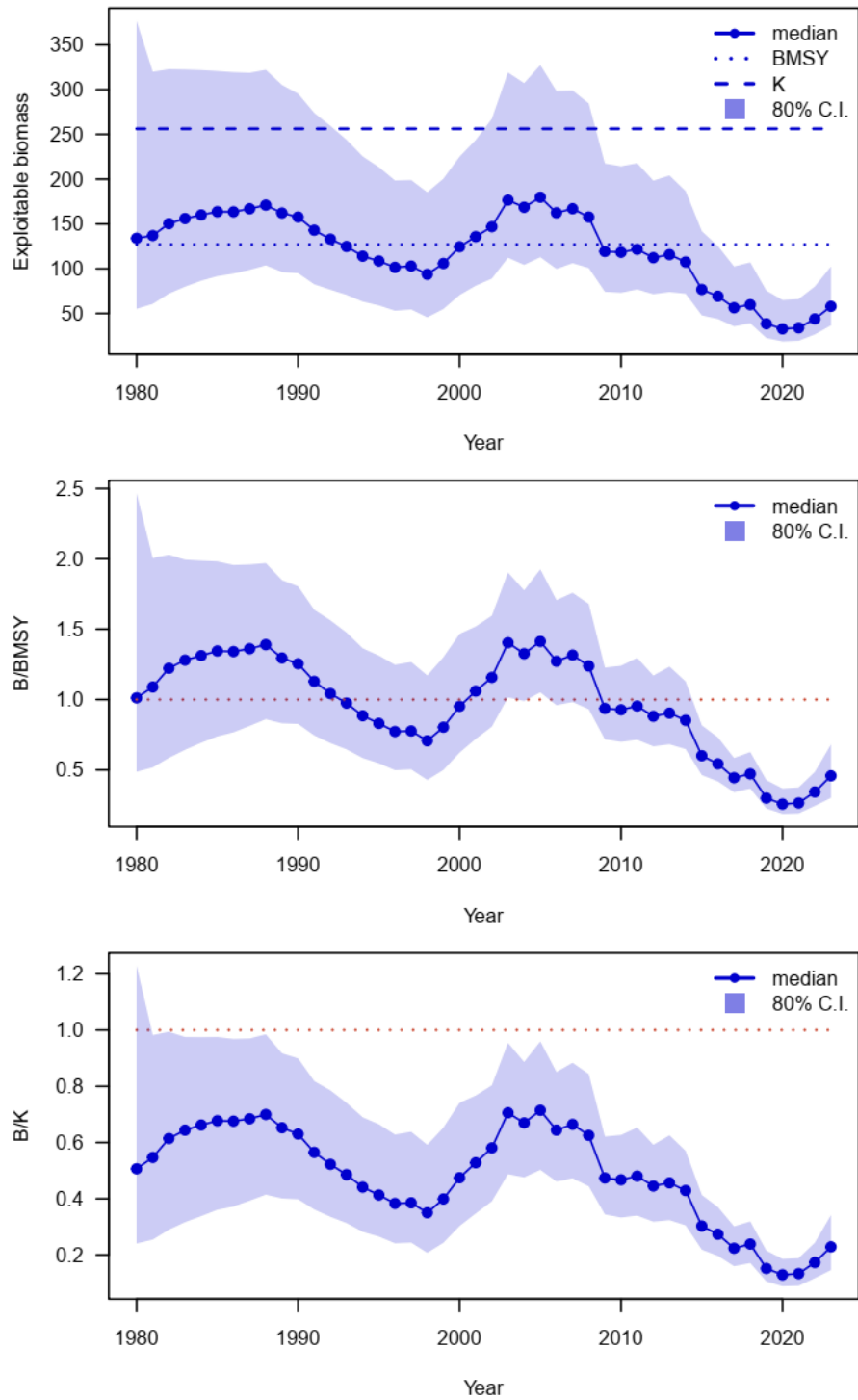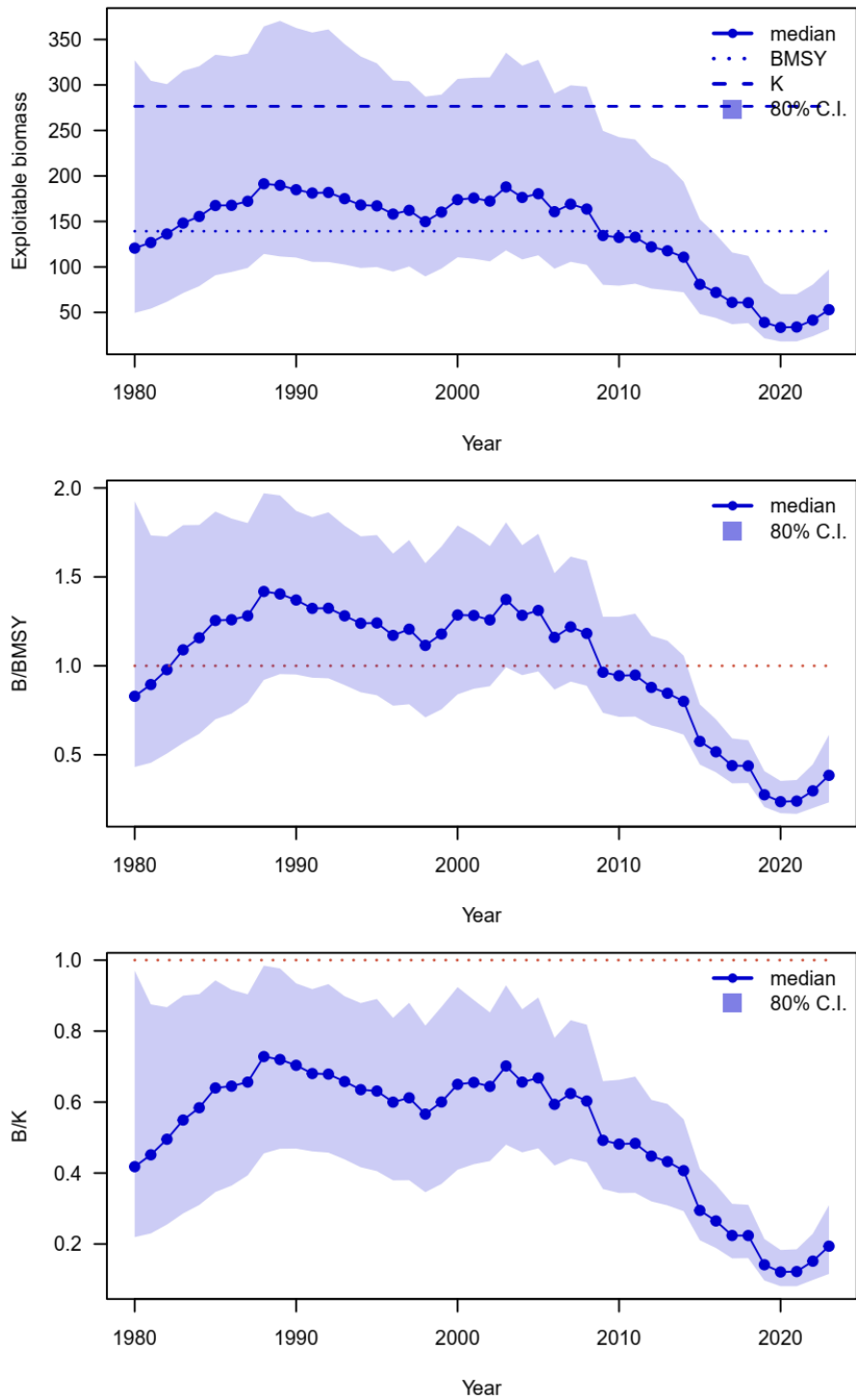
Figure A5. Time series of ensemble biomass (10,000 metric ton), the ratio of biomass to BMSY (B/B_{MSY}), and the depletion ratio (B/K) of the western North Pacific saury for the median estimates of MCMC results from base case1.
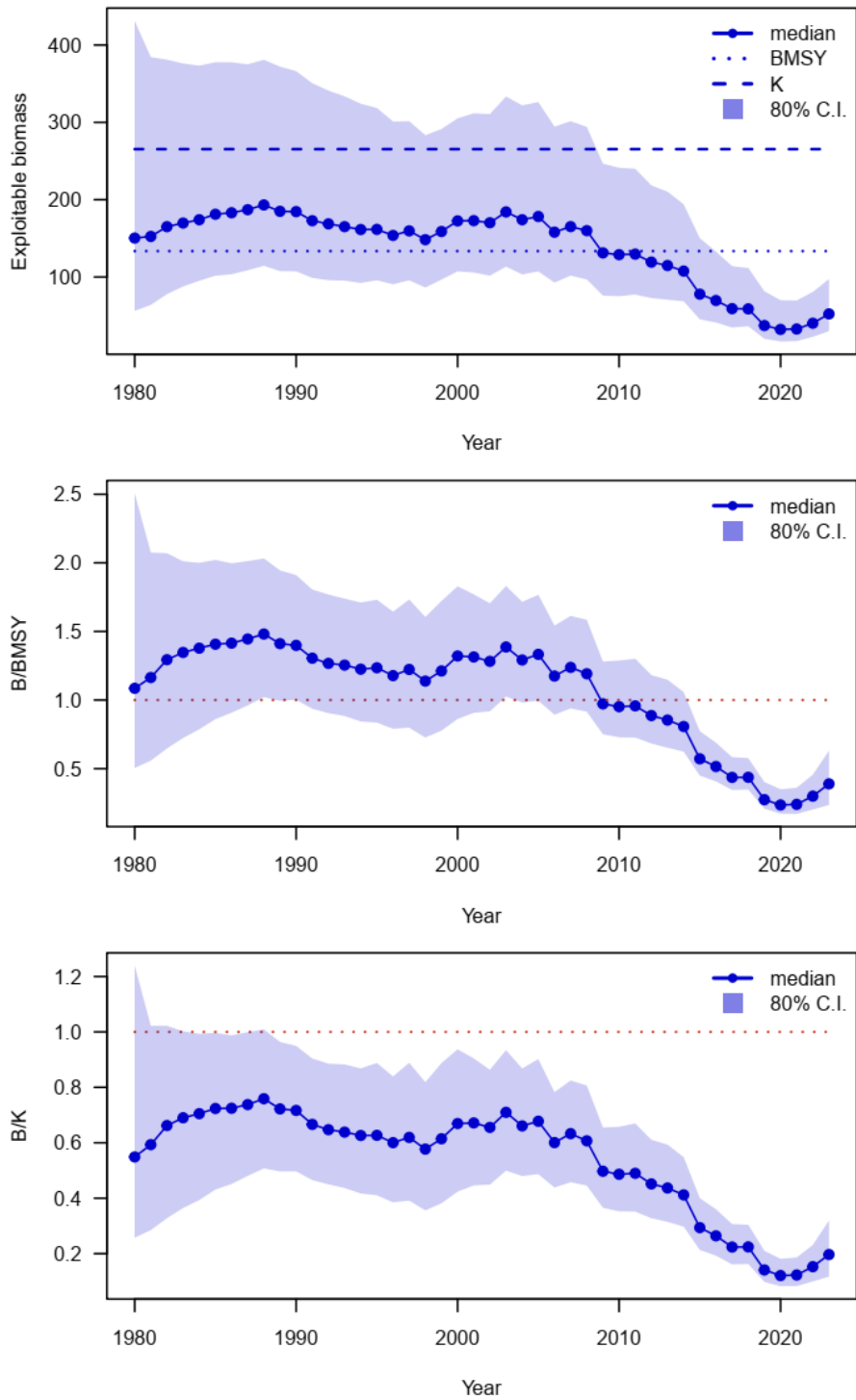
Figure A6. Time series of ensemble biomass (10,000 metric ton), the ratio of biomass to BMSY (B/BMSY), and the depletion ratio (B/K) of the western North Pacific saury for the median estimates of MCMC results from base case2.
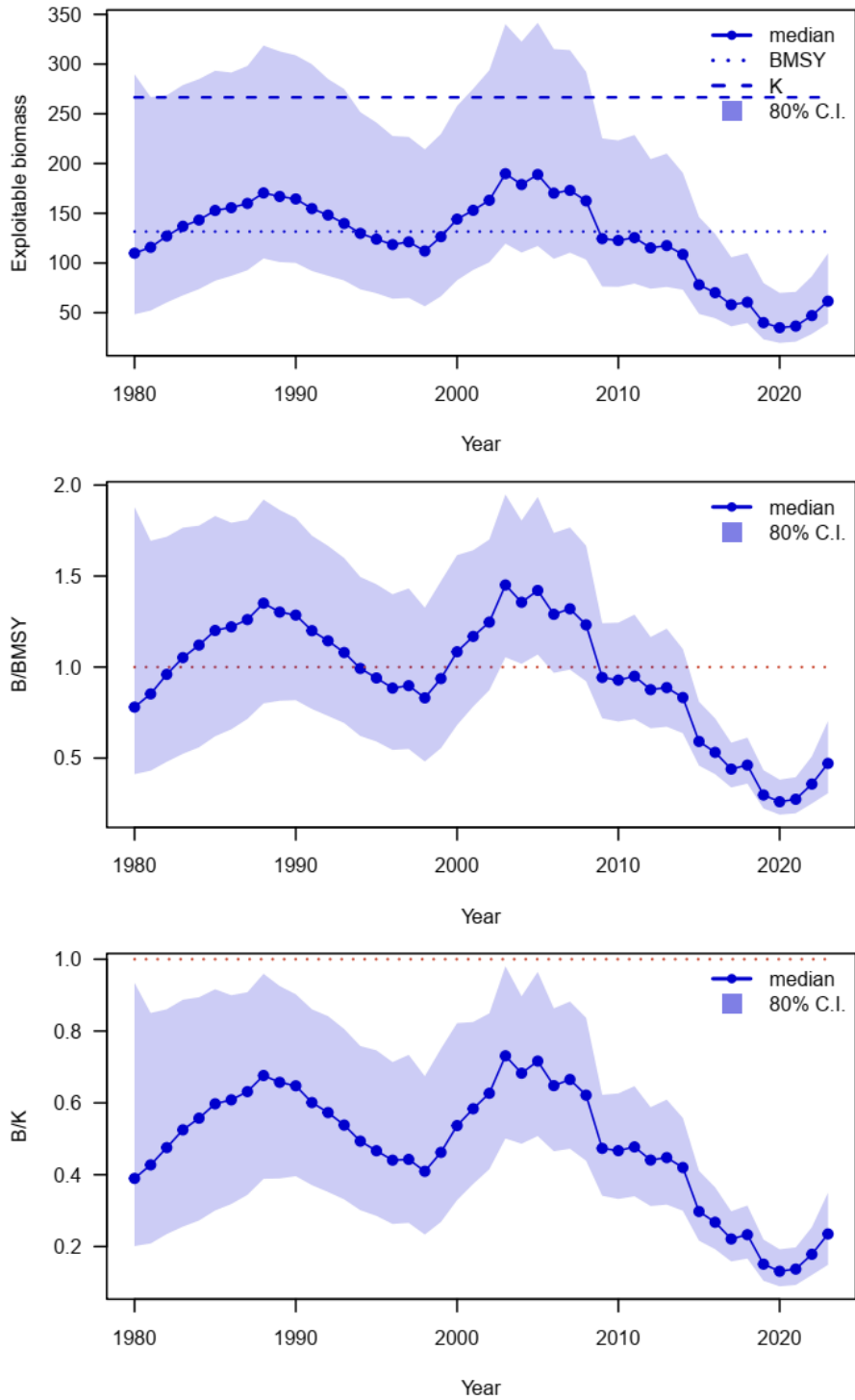
Figure A7. Time series of ensemble biomass (10,000 metric ton), the ratio of biomass to BMSY (B/BMSY), and the depletion ratio (B/K) of the western North Pacific saury for the median estimates of MCMC results from sensitivity case1.

Figure A8. Time series of ensemble biomass (10,000 metric ton), the ratio of biomass to BMSY (B/BMSY), and the depletion ratio (B/K) of the western North Pacific saury for the median estimates of MCMC results from sensitivity case2.
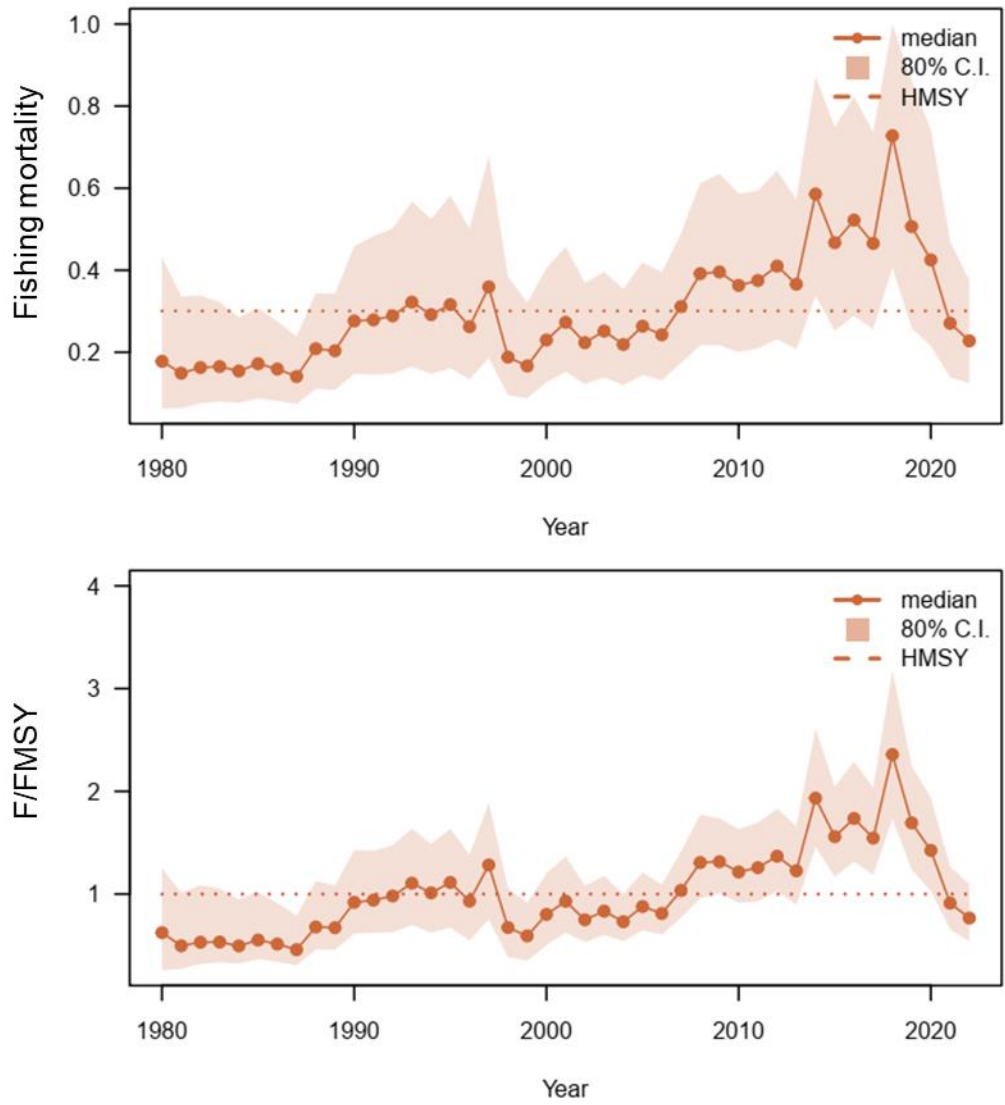
Figure A9. Time series of harvest rate and the ratio of harvest rate to HMSY (H/HMSY) (b) of the western North Pacific saury for the median estimates of MCMC results from base case 1.
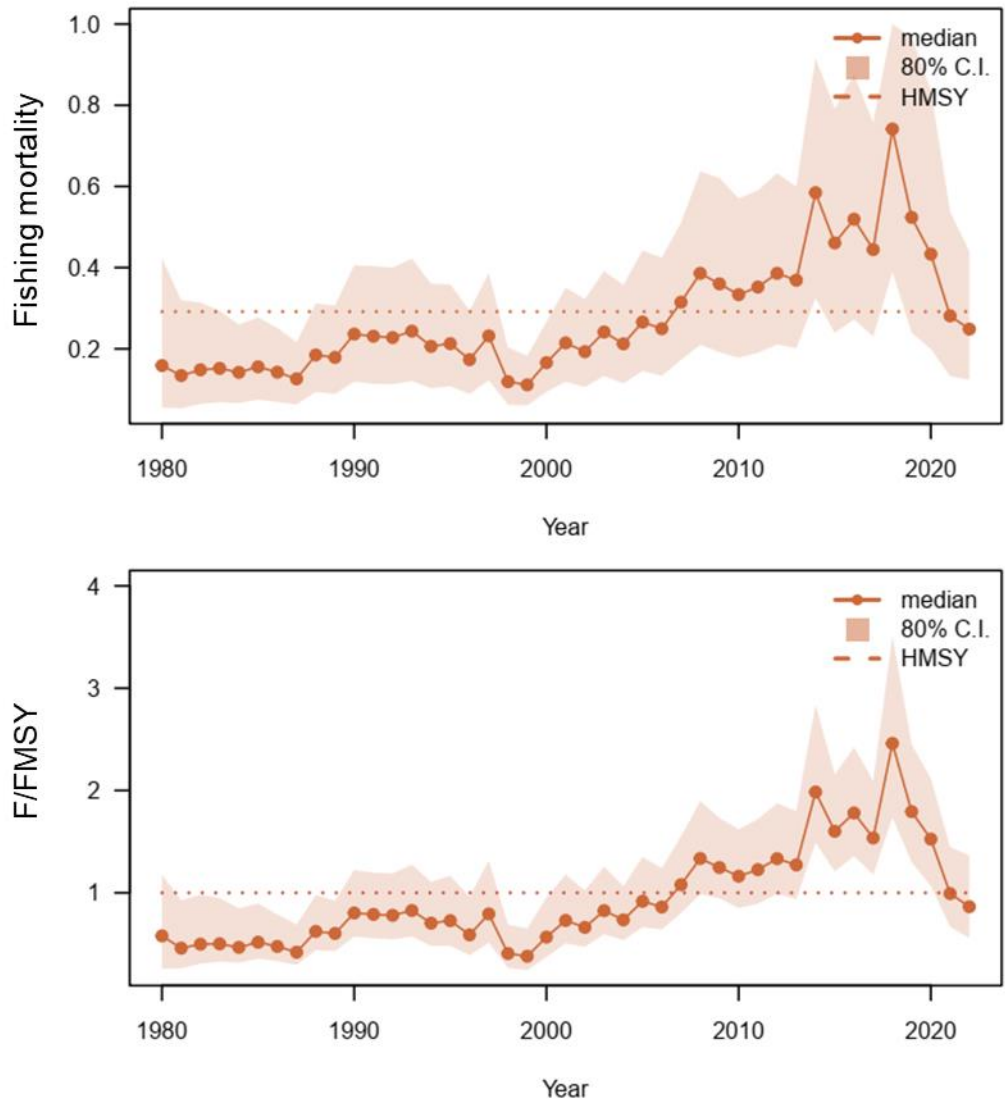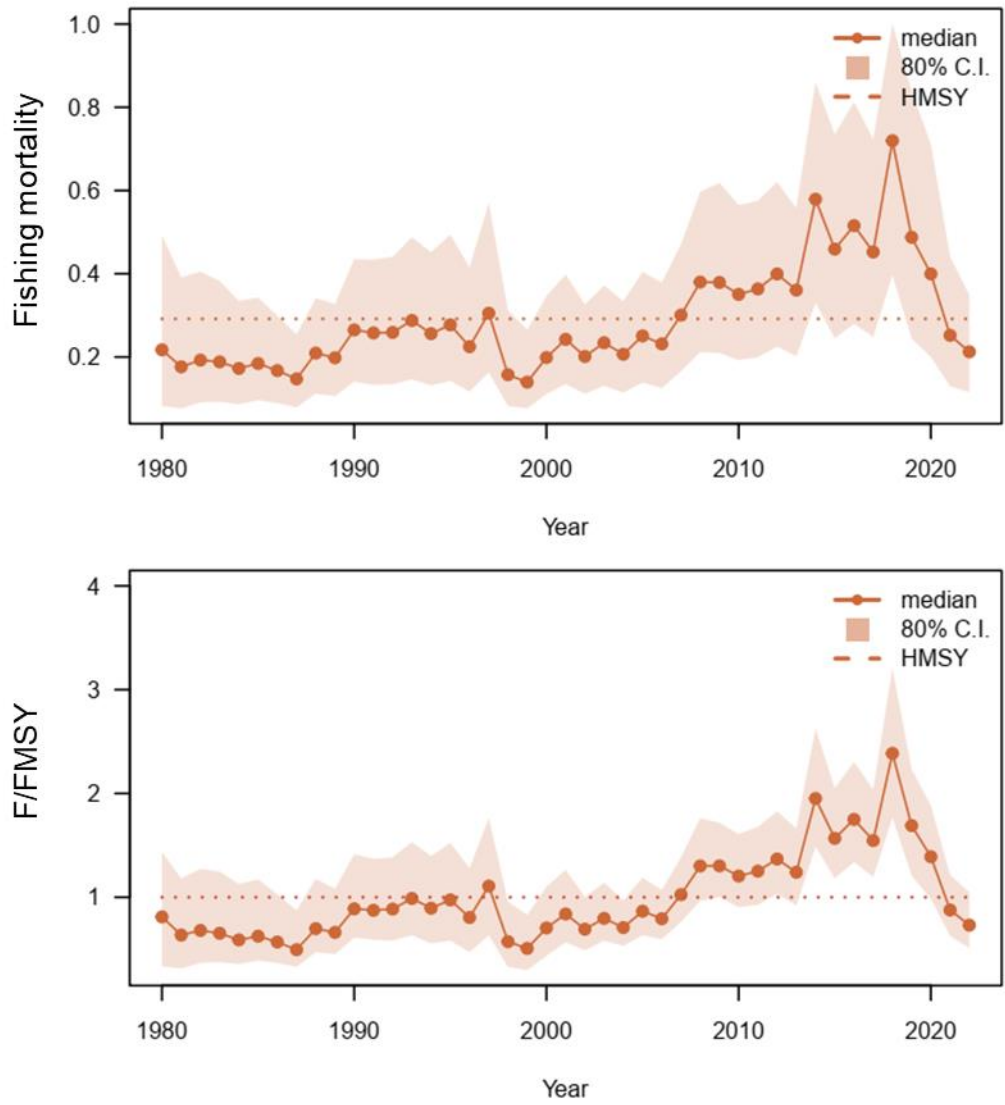
Figure A10. Time series of harvest rate and the ratio of harvest rate to HMSY (H/HMSY) (b) of the western North Pacific saury for the median estimates of MCMC results from base case 2

Figure A11. Time series of harvest rate and the ratio of harvest rate to HMSY (H/HMSY) (b) of the western North Pacific saury for the median estimates of MCMC results from sensitivity case 1.
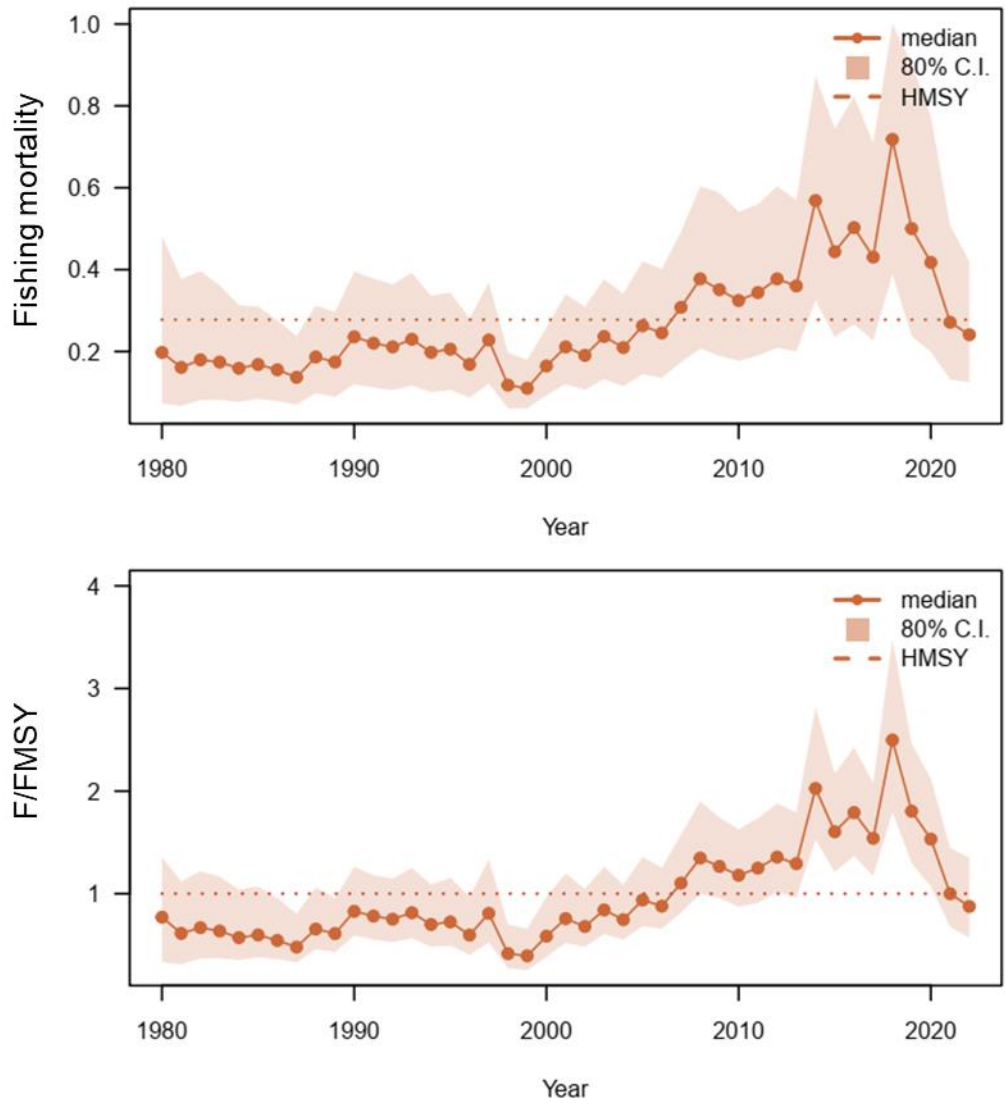
Figure A12. Time series of harvest rate and the ratio of harvest rate to HMSY (H/HMSY) (b) of the western North Pacific saury for the median estimates of MCMC results from sensitivity case 2.
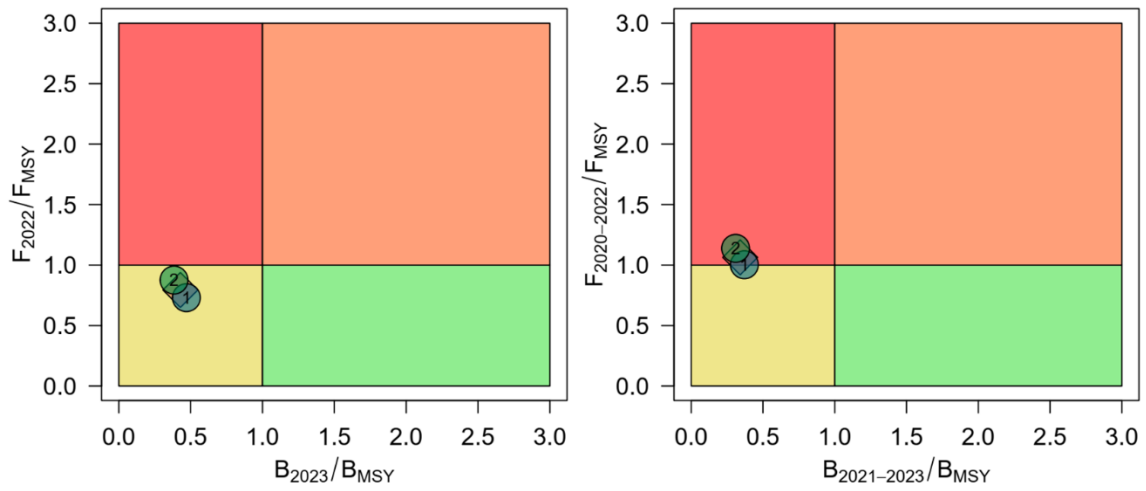
Figure A13. Kobe phase plot of stock status in the last year and recent three years (B2021 – 2023 and F2020 – 2022) of Pacific saury from the two base case models. The orange diamond is the median estimate of MCMC results from the two base case models.